Evolving Earth 4 (2026) 100124

Contents lists available at ScienceDirect

Evolving Earth

journal homepage: www.sciencedirect.com/journal/evolving-earth

Evolution of high latitude fluvial system in a humid climate conditions (Maastrichtian–Danian, Magallanes Basin, Chilean Patagonia)

Leslie M.E. Manríquez [a,*], Ernesto L.C. Lavina [b], Juan Pablo Pino [c], Cristine Trevisan [a,d], Jhonatan Alarcón-Muñoz [c,d,e], Joseline Manfroi [f,g], Hector Mansilla [a], Marcelo Leppe [d,h]

[a] Antarctic and Patagonia Paleobiology Laboratory, Instituto Antártico Chileno-INACH, Plaza Muñoz Gamero 1055, Punta Arenas, Chile
[b] Geology Graduate Program, Vale do Rio dos Sinos University, Av. Unisinos 950, 93022- 000, São Leopoldo, Rio Grande do Sul, Brazil
[c] Red Paleontológica UChile, Laboratorio de Ontogenia y Filogenia, Las Palmeras 3425, Ñuñoa, Santiago, Chile
[d] Evolutionary Transitions of Early Mammals Millennium Nucleus (EVOTEM), Chile
[e] Museo Nacional de Historia Natural, Interior Parque Quinta Normal s/n, Santiago, Chile
[f] Center of Research and Advancement of Paleontology and Natural History of Atacama (CIAHN), Prat 58, Caldera, Atacama, Chile
[g] Department of Biology, Paleontology Laboratory of Ribeirão Preto, Universidade de São Paulo - USP, São Paulo, Brazil
[h] GEMA Centre, Universidad Mayor, Santiago, Chile

ARTICLE INFO

Keywords:
Point bar deposits
Longitudinal bar deposits
Crevasse splay density flow
Taphonomy signature
Paleovertebrates
Paleobotany

ABSTRACT

This study documents fluvial dynamics and paleoenvironmental evolution in a high-latitude foreland basin during the Maastrichtian–Danian, based on integrated sedimentological and paleontological analysis of a continental–coastal succession exposed in the Río de las Chinas Valley, Magallanes Basin, southern Chile. The fluvial record is characterized by sandy to gravelly channel bodies embedded within an extensive muddy floodplain, reflecting deposition on a low-gradient fluvial plain developed in the distal sector of the basin. Two main channel styles are recognized within the fluvial system: sinuous channels dominated by lateral-accretion point-bar deposits, and higher-energy braided channels composed of sandy to gravelly longitudinal bars. These channel styles occur laterally within the same fluvial corridor, indicating that channel morphology was primarily controlled by spatial variability in sediment supply and discharge rather than by downstream changes in slope or base level alone. Gravel-rich braided reaches are interpreted to reflect higher bedload input, whereas sandy sinuous channels developed in sectors dominated by suspended load. Dispersed paleocurrent patterns are interpreted as the result of channel migration and bar accretion processes within a low-gradient system, rather than evidence for independent drainage networks. Floodplain deposits record frequent overbank flooding, crevasse-splay activity, abandoned channels, and swampy environments, locally including deposits related to hyperconcentrated flows generated during high-magnitude floods under humid climatic conditions. Recurrent vertical and lateral intercalations of fluvial and shallow-marine facies indicate direct interaction between fluvial systems and a high-energy, linear coastline, emphasizing the role of accommodation changes linked to relative sea-level fluctuations at the end of the Cretaceous. Paleobotanical and taphonomic evidence supports humid conditions during the Maastrichtian, followed by a shift toward cooler and drier climates near the Cretaceous–Paleogene transition. Overall, the Río de las Chinas succession provides a well-exposed record of fluvial dynamics in a high-latitude foreland basin at the end of the Cretaceous.

1. Introduction

Continental depositional systems are commonly classified according to the relative influence of fluvial, wave, and tidal processes, which together control sediment transport, accommodation, and facies distribution along basin margins (Galloway, 1975; Boyd et al., 1992; Dalrymple et al., 1992; Ainsworth et al., 2011). Within foreland basins, non-marine depositional systems are particularly sensitive to tectonic

* Corresponding author.
E-mail addresses: less.manriquez@gmail.com (L.M.E. Manríquez), lavina@unisinos.br (E.L.C. Lavina), juanpablo.pinomorales@gmail.com (J.P. Pino), ctrevisan@inach.cl (C. Trevisan), jhoalarc@gmail.cl (J. Alarcón-Muñoz), joselinemanfroi@ciahn.cl (J. Manfroi), hmansilla@inach.cl (H. Mansilla), mleppe@umayor.cl (M. Leppe).

https://doi.org/10.1016/j.eve.2026.100124
Received 27 November 2025; Received in revised form 19 March 2026; Accepted 1 April 2026
Available online 1 April 2026

subsidence, sediment supply from adjacent orogenic belts, and climatic variability, which together regulate fluvial discharge, channel patterns, and sediment load (Catuneanu et al., 2009). Although the stratigraphic record of foreland basins reflects the combined effects of tectonism, magmatism, climate, and relative sea-level changes at active continental margins (DeCelles, 2012; Condie, 2016; Horton, 2018), the relative role of marine controls on continental fluvial systems, especially during coastal–continental transitions, remains incompletely understood, particularly in high-latitude foreland basins where fluvial systems interact repeatedly with shallow marine environments.

The Magallanes/Austral Basin is a high latitude foreland basin that has been the subject of extensive geological research, largely focused on its marine stratigraphy and basin-scale sedimentary evolution (Arbe and Hechem, 1984; Biddle et al., 1986; Macellari et al., 1989; Malkowski et al., 2017; Moyano-Paz et al., 2018). Upper Cretaceous successions in the basin include deep-to shallow-marine deposits as well as coastal facies (Mella, 2001; Tettamanti et al., 2018). However, despite the wide extent of continental and coastal outcrops, fluvial systems, particularly those of the Dorotea Formation and related Upper Cretaceous continental units, have received comparatively limited attention, especially with respect to their internal architecture, channel morphology, and depositional organization (Leppe et al., 2012; Tettamanti et al., 2018; Moyano-Paz et al., 2018; 2021; Chimento et al., 2020).

In this work, we address this knowledge gap by examining a fossil-

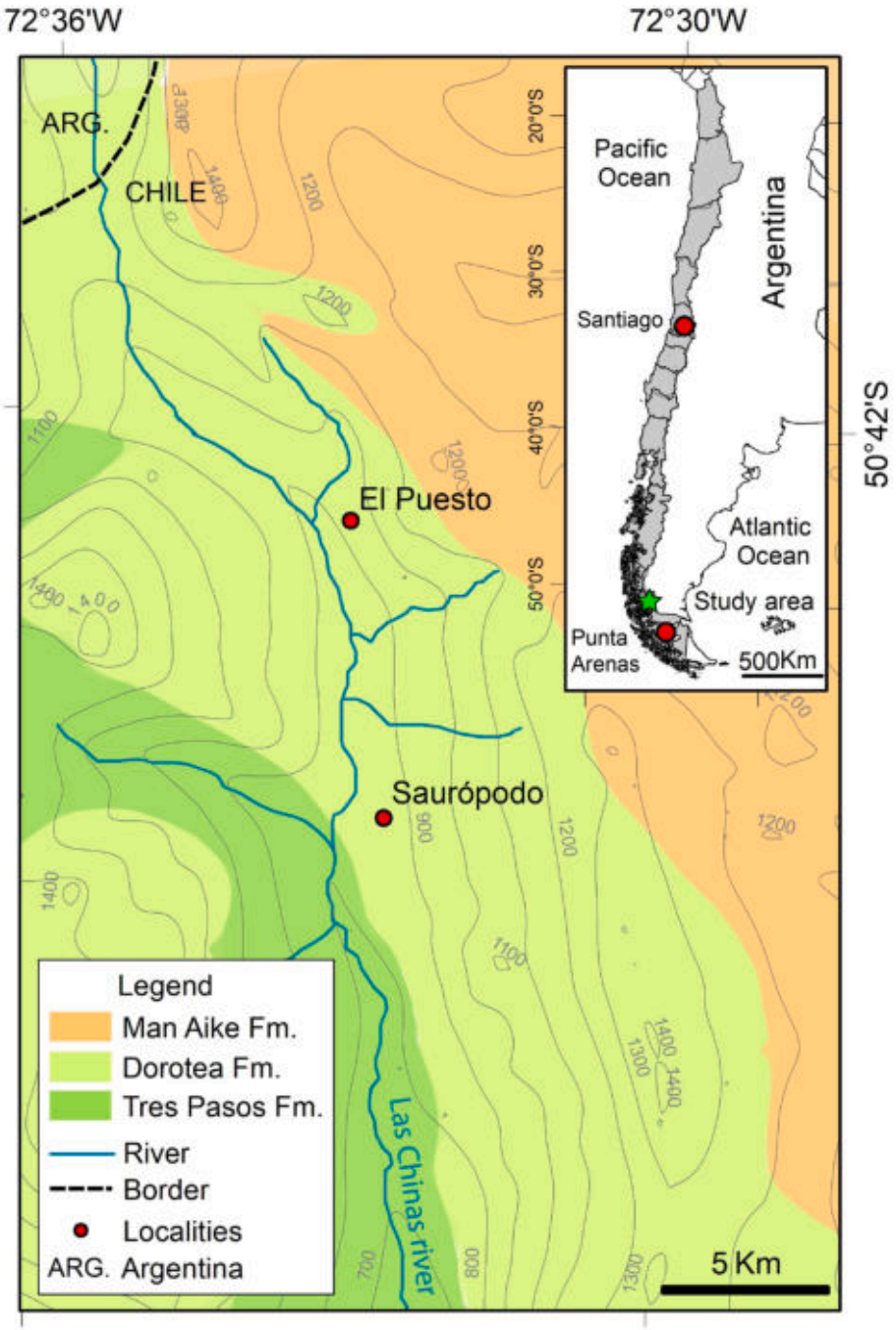

Fig. 1. Distribution of the Magallanes Basin formations (Tres Pasos, Dorotea, and Man Aike Formations) in the north of Río de las Chinas Valley. The studied localities corresponding to "El Puesto" and "Saurópodo" have been represented. In addition, the general map of Chile highlights the location of the Río de las Chinas Valley.

rich Upper Cretaceous fluvial succession from the Magallanes/Austral Basin using an integrated sedimentological and paleontological approach. The working hypothesis of this study is that fluvial deposits in high-latitude foreland basins record complex depositional architectures that reflect both upstream sediment supply and downstream marine influence. The main objective of this work is to characterize the depositional style and organization of these continental systems. Specific objectives include: (i) describing fluvial facies and channel architectures to constrain fluvial style and sediment dispersal patterns; (ii) evaluating the relationship between fluvial deposits and adjacent shallow-marine environments; and (iii) using paleobotanical assemblages to infer climatic conditions during the Late Cretaceous. Together, these objectives aim to improve our understanding of continental depositional systems and their controlling factors in high-latitude foreland basin settings.

2. Material and methods

In order to address the objectives outlined in the introduction, a study area was defined and an integrated methodological approach was designed to investigate the sedimentological, stratigraphic, and paleontological characteristics of the studied deposits. This approach combines detailed field-based sedimentological analyses with paleontological, taphonomic, and palynological studies, allowing for a comprehensive reconstruction of the depositional environments and fossil assemblages within a stratigraphic framework that explicitly considers fluvial-marine interactions.

The studied area is in the Río de las Chinas Valley, approximately 350 km north of Punta Arenas, Última Esperanza Province, in the Magallanes Region, Chile (Fig. 1). Geological and paleontological analyses were made in two sites located at the eastern flank of the Río de las Chinas Valley: “El Puesto” and “Saurópodo”. These localities were selected due to their excellent exposure of laterally continuous continental-coastal sucessions and their stratigraphic overlap within Upper Cretaceous depositional sequences.

A total of 12 stratigraphic sections, ranging from 20 to 200 m in thickness, were measured and logged across the two study areas. These sections were subsequently integrated into a composite stratigraphic section approximately 750 m thick. Lateral correlation between the El Puesto and Saurópodo sections was established using a combination of stratigraphic criteria, including the identification of regionally traceable marker beds, distinctive lithological packages, bounding surfaces associated with transgressive and regressive events, and overall stacking patterns of facies associations. Correlations were further supported by the relative stratigraphic position of key marine and continental facies and by spatial analysis using high-resolution satellite imagery (Google Earth). This integrated approach allowed the construction of a single composite stratigraphic section that captures both vertical and lateral variability of the fluvial and coastal systems, rather than relying solely on channel-scale correlations. Stratigraphic sections and associated photographic documentation were prepared using Adobe Illustrator CC software. Paleocurrent measurements (n = 233) were obtained from trough cross-bedding in point-bar and longitudinal-bar deposits and are presented as rose diagrams.

Fieldwork included detailed descriptions of lithology, bed geometry, thicknesses, sedimentary structures, mean grain size, sorting, paleocurrent measurements, fossil content and taphonomic data. Facies characterizations were based on the descriptions of Miall (2000). Facies associations are explicitly defined in this study as recurrent, genetically related groupings of facies that reflect specific depositional sub-environments (e.g., channel fills, floodplain deposits, crevasse splays, and coastal plain settings). The criteria used to define facies associations include lithology, sedimentary structures, architectural elements, paleocurrent patterns, fossil content, and taphonomic attributes.

The analysis of fluvial deposits was conducted within a sequence-stratigraphic framework, explicitly accounting for the presence of multiple depositional sequences and the repeated juxtaposition of fluvial, coastal plain, and shallow-marine facies. The nomenclature of depositional sequences follows Manríquez et al. (2019), with particular emphasis on sequences 3, 4, 5, and 6 (Fig. 2). Rather than treating the fluvial system as a single uninterrupted entity, fluvial facies and architectures were analyzed in relation to bounding surfaces and changes in accommodation associated with relative sea-level fluctuations. This approach allows evaluation of how marine transgressions and regressions influenced fluvial style, channel preservation, and floodplain development through time.

The fossils discussed in this study were collected during paleontological expeditions in the Río de las Chinas Valley, Chilean Patagonia. These fossils correspond to specimens of plants and vertebrates that are currently deposited in the Paleontological Collection of Patagonia and Antarctica (CPAP) at the Instituto Antártico Chileno (INACH), located in Punta Arenas, Magallanes Region, Chile and also in the Paleontology Collection of the National Museum of Natural History (MNHN) in Santiago, Chile. Taphonomic analyses of the fossil macroflora assemblage recovered during the paleontological expeditions were carried out based on morphological and systematic descriptions of fossil leaves and plant fragments, using the methodology and nomenclature of Greenwood (1991) and Gastaldo (2001). In addition, palynological analyses were also carried out at two sites (Fig. 1), where the sediments were processed using standard methodology for extracting and preparing palynomorphs (Wood et al., 1996; Jones and Rowe, 1999). The palynological slides were analyzed using a Carl Zeiss Axioscope 40X optical microscope and photographs were taken with a Cannon A740 camera. The palynological preparation residues were permanently mounted on slides and stored in the CPAP - INACH collection. Vertebrate fossils found in surface layers at different locations in the Río de las Chinas Valley were also corroborated with the taphonomic analyses.

3. Geological setting

The Magallanes/Austral foreland basin developed during the Late Jurassic to Early Cretaceous (Natland et al., 1974; Wilson, 1991; Fildani et al., 2003; Malkowski et al., 2017; Cuitiño et al., 2019), in association with rifting related to the breakup of Gondwana (Cuitiño et al., 2019), and the opening of the South Atlantic Ocean (Biddle et al., 1986; Harambour and Soffia, 1988; Mella, 2001). The basin covers part of the Chilean provinces of Última Esperanza and Magallanes, and the Argentine provinces of Santa Cruz and Tierra del Fuego (Mella, 2001; Ghiglione et al., 2009; Tettamanti et al., 2018; Varela et al., 2019). The basin has up to 8000 m of sediment at the depocenter. Its filling started with deep water marine deposits (turbiditic systems) and evolved into coastal and continental environments (Mella, 2001; Tettamanti et al., 2018).

In Santa Cruz province (Argentina), the uppermost continental Cretaceous deposits are exposed in the southwestern sector, associated to the Chorrillo, La Irene, and Cerro Fortaleza formations (Macellari et al., 1989; Tettamanti et al., 2018; Moyano-Paz et al., 2021). These deposits are interpreted as a product of meandering and braided fluvial systems (Tettamanti et al., 2018; Varela et al., 2019; Moyano-Paz et al., 2022).

In Chile, the upper Campanian to Danian deposits (Dorotea Formation) are 1250 m thick. These deposits originated in shallow marine and continental environments (Covault et al., 2009; Hubbard et al., 2010; Schwartz and Graham, 2015; Schwartz et al., 2016; Gutiérrez et al., 2017; George et al., 2020; Manríquez et al., 2019; 2021; Fosdick et al., 2020; Rivera et al., 2020). The fossil record of the Dorotea Formation includes abundant marine invertebrates (bivalves, ammonites, gastropods) and vertebrate remains (non-avian dinosaurs, birds, turtles, frogs, mammals, sharks, and marine reptiles) as well as, fossil plants (leaves and trunks) (Katz, 1963; Cortés, 1964; Schwartz and Graham, 2015; Manríquez et al., 2019, 2021; Trevisan et al., 2020; Alarcón-Muñoz et al., 2020, 2023; Goin et al., 2020; Martinelli et al., 2021; Suazo and Gómez, 2021; Soto-Acuña et al., 2021; Davis et al., 2023; Martínez et al.,

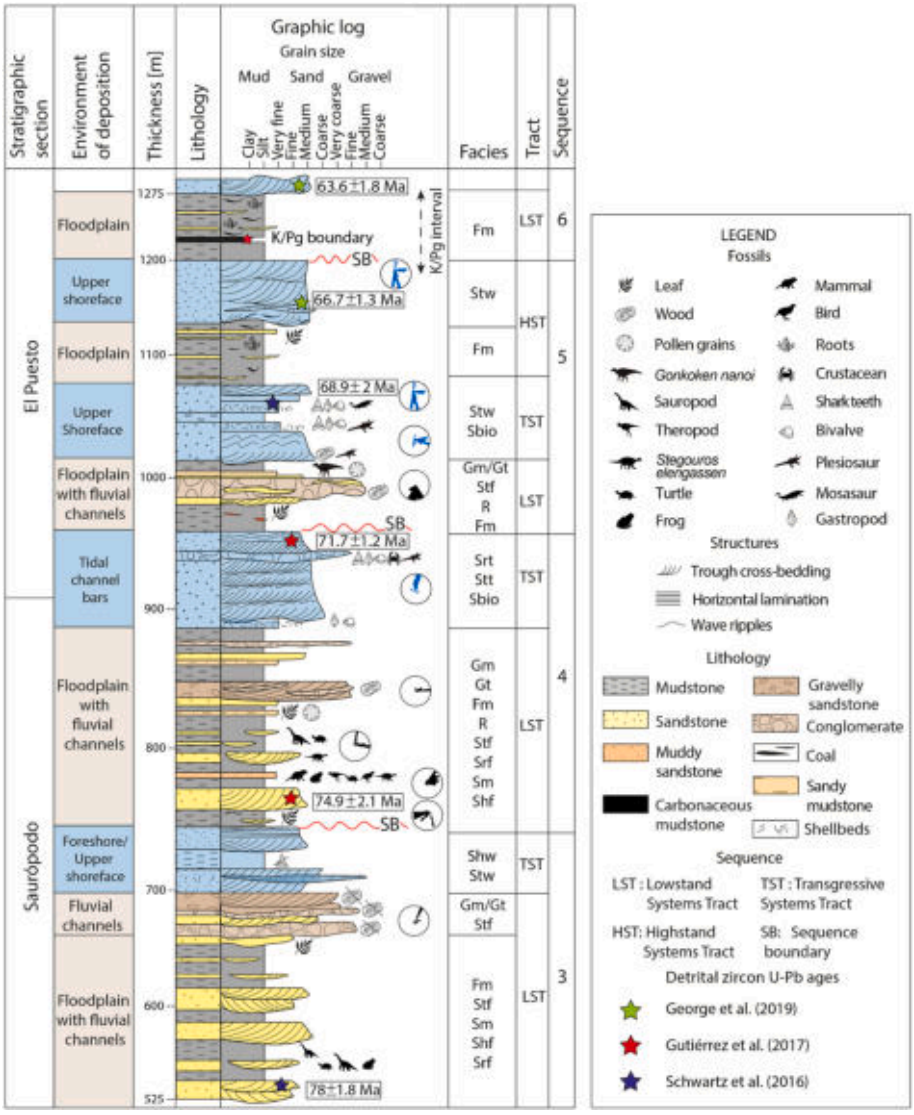

Fig. 2. General stratigraphy column with the depositional sequences, systems tracts, facies and depositional environments. The continental levels of the Río de las Chinas Valley (modified from Manríquez et al., 2019, 2021) are highlighted with colors.

2023; Püschel et al., 2025).

In the Río de las Chinas valley several vertebrates were also collected in continental deposits, including sauropod, theropod, and ornithischian dinosaurs, such as the hadrosauroid *Gonkoken nanoi* (Soto-Acuña et al., 2014, 2016a; Atisha-González et al., 2022; Bravo-Ortiz et al., 2022; Amudeo-Plaza et al., 2022; Davis et al., 2023; Alarcón-Muñoz et al., 2023). Among the ornithischians, the discovery of *Stegouros elengassen* stands out, as it represents the first species of ankylosaur named in South America (Soto-Acuña et al., 2021). In addition, finds of freshwater turtles (Alarcón-Muñoz et al., 2020), and the mammals *Magallanodon baikashkenke* (Goin et al., 2020), *Orretherium tzen* (Martinelli et al., 2021), and *Yeutherium pressor* (Püschel et al., 2025) have been reported.

The Dorotea Formation overlies the Tres Pasos Formation (Campanian; Romans et al., 2011; Auchter et al., 2016), and underlies the Man Aike Formation (Middle Eocene; Malumián, 1990; Camacho et al., 2000; Marenssi et al., 2003; George et al., 2020). Towards the top of the Dorotea Formation and under the Man Aike Formation there is a regional Paleogene unconformity developed throughout the basin. This unconformity has been previously interpreted as the product of widespread erosion due to Paleocene Patagonian Andes uplift (Biddle et al., 1986; Fosdick et al., 2011). In the Río de las Chinas Valley, the maximum depositional age was determined for the upper section of the Dorotea Formation, corresponding to 66 – 63 Ma interval (upper Maastrichtian to Danian; George et al., 2020), including the K/Pg boundary (Manríquez et al., 2024). Manríquez et al. (2019, 2021) recognized seven third-order depositional sequences in the Río de las Chinas Valley. Each sequence presents abrupt limits marking environmental changes from marine to continental deposits due to the relative sea-level base drop. The lowstand system tract (LST) is formed by continental facies, and transgressive and highstand system tracts (TST and HST) include marine facies, represented by foreshore, shoreface and offshore transition deposits (Manríquez et al., 2019).

4. Results

The studied area consists of a 750 m-thick sedimentary succession that contains 3 facies associations inside four third-order depositional sequences (Figs. 2 and 3). These continental facies (Table 1) are indicative of channel bars of braided and meandering rivers corresponding to 30% of deposits, while 70% of these deposits show a wide floodplain. These deposits are interpreted as a LST, as originally proposed by Manríquez et al. (2019). Additionally, continental deposits recognized within the HST indicate progradation and an increased continental influence during highstand conditions. The marine facies association were

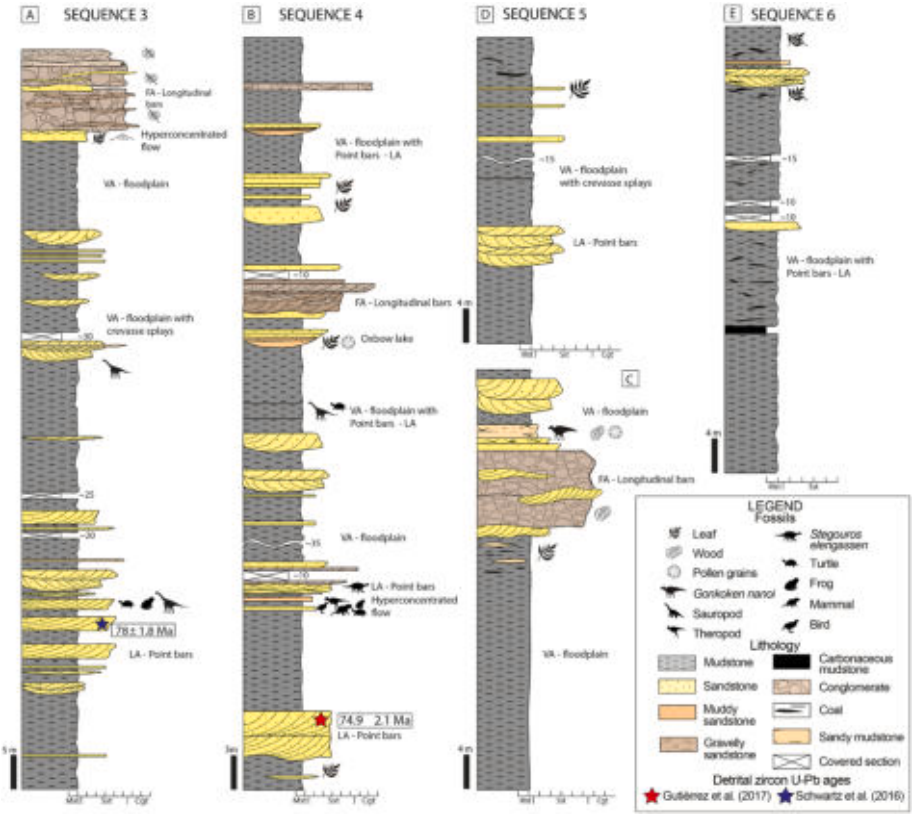

Fig. 3. Stratigraphic profile of the continental depositional sequences 3 to 6. (A-C) Stratigraphic profiles of sequences 3,4 and 5, showing the sinuous and braided channels within floodplain deposits (oxbow lake and crevasse splays). (D-E) Stratigraphic profiles of sequence 5 and 6 showing the wide mud floodplain with crevasse splays, swamp and scattered pointed bar deposits. Abbreviations: Mst: Mudstones, Sst: Sandtones, Ggt: Conglomerate, VA: vertical accretion, FA: frontal accretion, LA: lateral accretion.

described in Manríquez et al. (2021), and characterize the high-energy shallow marine deposits that intercalated with continental deposits. These deposits represent TST and HST, which indicate the wide upper shoreface and foreshore, and tidal channel deposits (Manríquez et al., 2019, 2021).

4.1. Facies association

4.1.1. Longitudinal bars facies association

4.1.1.1. Description. The longitudinal bars facies association consists of conglomerate and gravelly to coarse-grained sandstones (Gm, Gt, and Stf facies, Table 1). This facies association can form either continuous levels with a lateral extension more than 7 km long and up to 20 m-thick (measured longitudinally to the paleoflow direction), or several disconnected minor lenses (162 to 390 m-long by 5 to 10 m-thick) separated by floodplain mudstones (Figs. 4A and 1– see supplementary material). Internally, they are formed by lenticular beds of conglomerates and coarse sands poorly sorted and with normal grading. These beds are elongated/lenticular and separated by erosive surfaces with a low dip (<10°), coinciding with the direction of the medium to large -scale trough cross-beddings (0.3 to 1.5 m-thick). The conglomerate beds present imbricated clast, wood debris, and coarse-to medium-grained trough cross-bedding sandstone lenses (Fig. 4B, C, D). Paleocurrent data from trough cross-bedding in these facies indicate northeast, east, and southward sediment transport (Fig. 2).

4.1.1.2. Interpretation. The lenticular geometry, presence of coarse granulometry with trough cross-bedding, imbricated clasts, finning-upward cycles, and low paleocurrent dispersion pattern suggest that this facies association consists of channel bars of braided streams (Smith, 1984; Reinhardt et al., 1986; Scherer and Lavina, 2005, 2006). The coincidence between the erosive surfaces' dip angles, the associated cross-bedding's general direction, and the absence of sigmoidal surfaces, suggests frontal accretion and correspondence with longitudinal bar architectural elements (Harms et al., 1982; Ashmore, 1991; Eberth and Miall, 1991; Miall, 2000; Finzel and McCarthy, 2005; Scherer et al., 2007; Pyrcz, 2015). The conglomerate cycles ended with sandstone lenses at the top, are associated with frontal accretion at the top of the bars.

4.1.2. Point bar facies association

4.1.2.1. Description. The point bar facies association form large lenses up to 4 m-thick and 50 to 300 m long measured longitudinally to the paleoflow direction, always in erosive contact with the mudstone facies (Figs. 5B, 6A and 1- see supplementary material). They are formed by lenticular beds of fine grained to gravelly sandstones with medium to large-scale trough cross-bedding (0.5 to 1.4 m-thick) and massive granule/pebbles conglomerate lenses (Stf, Table 1, Figs. 5C and 6B, C, D). The sandstones present moderate to poorly sorted and normal grading. The diagnostic feature of these facies is the presence of inclined erosive surfaces with angles less than 20°. When this general inclination is compared with the trough cross-bedding direction, in the transverse sections to the flow, they present a general sigmoidal shape (Fig. 5B). In parallel cuts to the flow direction, they may show a slight upward convexity. Paleocurrent data from trough cross-bedding indicate north, northeast, east, south and southwestward sediment transport, along the succession (Fig. 2).

This facies is very fossiliferous. A *Stegouros elengassen* skeleton and isolated bones of sauropods, freshwater turtles (cf. *Yaminuechelys* sp.), and frogs were found (Fig. 7A; see Table 2 for details).

Table 1
Description and interpretation of continental and marine deposits of the Río de las Chinas Valley. Localities: El Puesto and Saurópodo. DP: Depositional sequences (Manríquez et al., 2019).

Facies code	Sedimentary facies	Sedimentary characteristics	Depositional processes	Environment
Fm	Massive mudstone	Greenish gray, yellowish brown, and dark gray mudstone. Massive to incipient horizontal lamination. Scarce thin lenses of fine grained sandstone. Locally, carbonaceous mudstones. Tabular beds and lenticular lenses. Organic matter. Load cast. Paleosols with rhizolites. Coal lenses. Plant fossils and vertebrates. Thickness: 0.2 to 20 m DP: 3,4,5 and 6	Suspension (Collinson, 1996; Schnurrenberger et al., 2003). Beadload (e.g., Wakelin-King and Webb, 2007; Wright and Marriott, 2007; Dasgupta et al., 2017). (Vertical accretion). Vegetated swamp deposits (Spackman, 1974; Cohen, 1984; Gleason and Stone, 1994; Miall, 1996; Orem and Finkelman, 2003)	Floodplain (Miall, 2000; Boggs, 2006; Nichols, 2009).
R	Rhythmite	Intercalation of whitish gray sandy mudstone and claystone. Coal lamina and muddy to very fine-grained sandstone lenses. Plant fossils and vertebrates. Thickness: 0.7 to 2.5 m DP: 4 and 5	Suspension (Le Hir et al., 2011; Talbot and Allen, 1996) (Vertical accretion)	Floodplain Oxbow lakes and lagoon (Miall, 2000; Nichols, 2009).
Srf	Ripple cross-lamination sandstones	Fine grained sandstones. Moderately sorted. Ripple cross-lamination. Laterally extended lenticular beds. Thickness: 0.1 to 0.5 m DP: 3 and 4	Suspension/bedload transport (Le Hir et al., 2011; Talbot and Allen, 1996) and lower flow regime (Miall, 2000).	Floodplain Crevasse-splay deposits – Natural breach levees (Miall, 2000). Unconfined flow.
Sm	Massive sandstones	Whitish-gray silty to medium -grained sandstones. Moderately sorted. (1) massive with scattered clast or (2) diffuse lamination with inverse and normal grading. Lenticular beds. Plant fossils and vertebrates. Thickness: 0.8 to 1.6 m DP: 4	Bedload transport (Le Hir et al., 2011; Talbot and Allen, 1996). Hyperconcentrated density flow (Drake, 1990; Miall, 2000; Mulder and Alexander, 2001) (1) Frictional shear regime: moderate shear stress rate, collision-free grain friction. (2) Collision shear regime: high shear stress rate, intense grain collision (traction carpets).	Floodplain Crevasse-splay deposits Mass flow associated with the rupture of natural levee (Hughes and Lewin, 1982; Miall, 2000, 2002; Nichols, 2009).
Shf	Horizontal lamination sandstones.	Whitish-gray silty to medium-grained sandstones. Moderately sorted. Horizontal lamination. Laterally extended lenticular beds. Local ripple cross-lamination sandstones. Plants fossils and vertebrates. Thickness: 0.3 to 1 m DP: 3 and 4	Suspension intercalated with bedload transport. Plane-bed flow (associated with low-energy turbulent flow) (Le Hir et al., 2011; Talbot and Allen, 1996).	Fluvial floodplain Crevasse-splay deposits – Natural breach levees (Miall, 2000). Unconfined flow
Stf	Trough cross-bedding sandstones	Fine to gravelly sandstones. Moderately to poorly sorted. Trough cross-bedding. Fine grained-conglomerate lenses. Lenticular beds. Finning-upward. Inclined erosive surfaces. (1) Internal, with irregular or inclined erosive surfaces (sigmoidal surfaces). DP: 3, 4 and 5. Thickness: 0.2 to 1.20 m; (2) Internally inclined erosive surface with small dip. DP: 3, 4 and 5. Thickness: 0.5 to 1.40 m. Vertebrates and wood fossil remains.	Bedload transport (Le Hir et al., 2011; Talbot and Allen, 1996). Unidirectional high-energy turbulent flow (Harms et al., 1982)	Channel deposits: 1) Lateral accretion; sinuous channel and crevasse channel (Miall, 2002). 2) Frontal accretion: braided channel (longitudinal bars) (Miall, 2000, Finzel and McCarthy, 2005).
Gt	Trough cross-bedding conglomerate	Clast-supported, poorly sorted, polymictic conglomerate (quartz, plagioclase and volcanic lithics). Clast size: 2 to 10 cm; modal size: 5 mm. Matrix is coarse- to very coarse-grained sandstone. The clasts are sub-discoidal to sub-prismoid, and sub-angular. Crudely horizontally stratified or massive sheets. Imbricated clasts. Finning-upward lenticular beds. Coarse to medium-grained sandstone lenses (St facies). Wood fossils. Thickness: 0.30 to 1.50 m DP: 3, 4 and 5	Unidirectional high-energy turbulent flow. (Ramos and Sopeña, 1983; Miall, 2000; Scherer et al., 2007). Bedload gravel deposited by clast-by-clast accretion during higher discharges (Finzel and McCarthy, 2005).	Braided channel-bar deposits Longitudinal bar (Ashmore, 1991; Eberth and Miall, 1991; Miall, 2000; Finzel and McCarthy, 2005; Scherer et al., 2007; Pyrcz, 2015).
Gm	Massive conglomerate	Clast-supported, poorly sorted, polymictic conglomerate (quartz, plagioclase and volcanic lithics). Clast size: 1 to 8 cm; modal size: 4 mm. Matrix is coarse- to very coarse-grained sandstone. The clasts are sub-discoidal to sub-prismoid. Imbricated clasts. Finning-upward lenticular beds. Coarse to medium-grained sandstone lenses (St facies). Wood fossils. Thickness: 0.20 to 1.20 m DP: 3, 4 and 5	Unidirectional high-energy turbulent flow. (Ramos and Sopeña, 1983; Miall, 2000; Scherer et al., 2007). Bedload gravel deposited by clast-by-clast accretion during higher discharges (Finzel and McCarthy, 2005).	Braided channel-bar deposits Longitudinal bar (Smith, 1984; Reinhardt et al., 1986; Miall, 2000; Scherer and Lavina, 2005, 2006).
Stw	Trough cross-bedding sandstones	Medium to very coarse-grained sandstone. Moderately to well-sorted. Medium scale trough cross-bedding, and locally massive.	Combined-flow dunes: unidirectional turbulent flow (Myrow and Southard, 1991; Kleinhans, 2004) associated with high energy wave action (	Upper shoreface (longshore drift) (McCubbin, 1982; Johnson and

(*continued on next page*)

Table 1 (*continued*)

Facies code	Sedimentary facies	Sedimentary characteristics	Depositional processes	Environment
		Associated with conglomerate lenses and thin extensive pebble sheets. Normal and inverse grading inside of the lamina. Thin coal lenses. Calcareous concretions. Elongated lenticular beds. Locally (sequence 5) ripple cross-lamination in medium-grained sandstone. Thickness: 1 m to 1.5 m DP: 3, 4, 5 and 6	McCubbin, 1982; Johnson and Baldwin, 1996; Reading and Collinson, 1996). Oscillatory asymmetric wave ripples (De Raaf et al., 1977)	Baldwin, 1996; Reading and Collinson, 1996).
Sbio	Fossil-rich sandstone	Medium-grained to gravelly sandstone. Moderately to poorly sorted. Abundant marine body fossil fragments. Massive. Locally medium scale trough cross bedding. Calcareous concretions. Elongated lenticular beds. Thickness: 0.05 to 0.3 m DP: 4	High-energy wave action (Myrow and Southard, 1991; Li and Amos, 1999) .	Breaker zone (transgressive wave-ravinement surfaces) (Myrow and Southard, 1991; Li and Amos, 1999)).
Shw	Medium to coarse-grained sandstone with horizontal lamination	Moderately to well-sorted; fine-grained conglomerate lenses. Horizontal lamination with low angle truncation. Lenticular units. Cone in cone. Thickness:0.2 to 10 m DP: 3	Upper flow regime (Van de Meene et al., 1996; Johnson and Baldwin, 1996)	Foreshore (Van de Meene et al., 1996; Johnson and Baldwin, 1996)
Fh	Mudstone, horizontal lamination	Dark, violet and gray. Marine invertebrates and vertebrates. Thickness: 7 to 10 m DP: 3	Suspension (Greenwood and Xu, 2001)	Offshore conditions (De Raaf et al., 1977; Greenwood and Xu, 2001).
Stt	Trough cross-bedding sandstones with flaser-bedding	Fine to medium-grained sandstones. Moderately-sorted. Medium scale trough cross-bedding with mud drapes and mud clasts on the foresets. Mud lamina. Thin beds (<10 cm) of rippled sand with mud drapes (flaser bedding). Elongated lenticular beds. Marine invertebrates and vertebrates. Thickness: 0.6 to 0.8 m. DP: 4	Combined-flow dunes: unidirectional turbulent flow (Myrow and Southard, 1991; Kleinhans, 2004) associated with oscillatory ripples. Mud drapes deposition during slackwater periods and lower-energy times (Klein, 1970; De Mowbray and Visser, 1984; Willis, 2005; Longhitano et al., 2012).	Tidal current in tidal channel (channel-bars) (De Mowbray and Visser, 1984; Longhitano et al., 2012).
Srt	Ripple cross-lamination sandstone	Medium grained sandstone. Moderately to well-sorted. Lenticular beds. Thickness: 0.3 m DP: 4	Oscillatory flow (De Raaf et al., 1977). Wave action on the upper part of tidal channel bars (Dalrymple and Choi, 2007; Longhitano et al., 2012)	Tidal channel bars (Dalrymple and Choi, 2007; Longhitano et al., 2012)

4.1.2.2. Interpretation. The lenticular sandstone bodies with normal grading, moderate-to poorly-sorted and trough cross-beddings have been attributed to deposition in migrating fluvial bars and channels (Reinhardt, 1980; Smith and King, 1983; Smith, 1984; Reinhardt et al., 1986). The inclined erosive surfaces with sigmoidal shapes in a transverse section (in relation to flow direction) correspond to lateral accretion surfaces (Miall, 2000; Willis and Tang, 2010). This geometry is associated with sinuous channels (meandering rivers) related to point bar architectural elements (Nanson and Croke, 1992; Smith et al., 2009; Willis and Tang, 2010; Durkin et al., 2020).

The Shf and Srf facies lenticular beds, which are directly connected to the upper part of the point bar deposits, correspond to the partial preservation of the natural levee deposits.

4.1.3. Floodplain facies association

4.1.3.1. Description. The floodplain facies association consists of massive mudstones (Fm) and rhythmite (R) facies (C; Table 1), associated with lenticular sandstones and with trough cross-beddings (Stf), tabular massive sandstones (Sm), and with ripple cross- and horizontal lamination sandstones (Srf and Shf). The massive mudstones (Fm) are the dominant lithology (Fig. 3), and are comprised of greenish gray, yellowish brown, and gray mudstones in 0.2 to 20 m-thick levels, and with a lateral extension of 5 km or more (Fig. 8A, B, E). Layers with Fe nodules and roots (rhizoliths) are relatively common. Lenticular intercalations of thin layers (1 to 5 mm) of claystone and whitish gray sandy siltstone (R facies) form packages up to 2.5 m thick and 10 to 30 m long (Fig. 8C). Inside the Stf, R and Fm facies there are thin carbon lenses. A 1 m-thick carbonaceous mudstone bed with at least 1 km of lateral extension is preserved in sequence 6 (Fm facies, Fig. 8D). In general, the Fm and R facies consist of tabular and lenticular beds with lateral extensions from a few hundred meters to 3 km.

Many levels of the Fm facies preserve abundant plant impressions, and disarticulated sauropod, anurans and turtle bones (Figs. 2 and 3). The R facies has palynological content, abundant plant impressions (tree branches, stems, roots, and leaves), remains of trunks such as *Austroginkgoxylon dutrae*, *Agathoxylon antarcticum*, *Podocarpoxylon paradoxi*, *Podocarpoxylon mazzonii*, *Palmoxylon subantarcticae* and *Notomalvaceoxylon magallanense*, and dinosaur remains such as *Gonkoken nanoi* bones (Tables 1 and 2).

4.1.3.2. Interpretation. The mudstone deposits are products of suspension processes (Collinson, 1996; Bridge, 2006) and substantial fraction of the mud is transported and deposited as traction load (e.g., Wakelin-King and Webb, 2007; Wright and Marriott, 2007; Dasgupta et al., 2017). The environmental context highlights the presence of abundant plant fragments and bones of terrestrial vertebrates, as well as large sandy and gravelly lenses (Stf and Gt facies) associated with sinuous and braided channels, features that allow its association with floodplain deposits. Muddy facies are related to channel overflow during rainy periods (and, although less likely in a warmer period, spring thaw), where fine sediments are deposited (Marzo, 1992). These fine sediments are carried in suspension by the flood waters and distributed over broad plains lateral to the channels, constituting different sub-environments. As flow decelerates, the fine sediments are deposited as bedload (Wakelin-King and Webb, 2007). Deposition from overbank waters

Fig. 4. Longitudinal bars facies association. (A) Elongated lenticular units of conglomerates (Gm facies) separated by floodplain mudstones (vertical accretion, Fm facies). (B) Conglomerate beds with very coarse-grained sandstone lenses, with trough cross-bedding (St facies associated), and with erosive contact between Gt facies and Fm facies. (C) Detailed image of massive conglomerate. (D) Gravelly sandstone levels with trough cross-bedding. Abbreviations: VA: vertical accretion, FA: frontal accretion.

results in sediment up building by vertical accretion (Miall, 2000). The presence of discrete root horizons (rhizoliths) is associated with poorly developed paleosols (Retallack, 2001). Gray colors and the presence of Fe/Mn nodules indicate reductive conditions in soils located in low zones, possibly water-logged (Retallack, 2001). Rhythmite lenses correspond to both temporary lagoons and abandoned channel (oxbow lake) deposits (Smith, 1984; Miall, 2000; Boggs, 2006). Lagoon deposits tend to be thinner and more elongated while abandoned channel deposits are narrower and thicker (up to 1.5 m).

4.1.3.3. Levee and crevasse splay deposits

4.1.3.3.1. Description. The deposits consist of horizontal lamination (Shf), ripple cross-lamination (Srf), massive (Sm), and trough cross-bedding (Stf) sandstones (Fig. 9A, B, C; Table 1). They have lenticular geometry, and its thickness varies from a few centimeters to 1.6 m.

The Shf and Srf facies occur as very extended lenses within the Fm facies, and on top of the Stf facies associated with sigmoidal erosive surfaces (point bar deposits). At the top of the point bars, they form accumulations up to 70 cm thick. When intercalated with the floodplain mudstones, but still close to the channels, the Shf and Srf facies form lenticular layers up to 30 m long and 20 to 70 cm thick (Fig. 5A–D).

The Sm facies occur in two distinct contexts: (1) massive beds of silty to fine-grained sandstones with dispersed granules, small pebbles, and organic clasts, and (2) presenting a diffuse lamination formed by laminae with normal and inverse grading (Fig. 9D and E). An exotic element characteristic of this facies is the presence of scattered bones of reptiles, non-avian dinosaurs, birds, frogs, and mammals (Fig. 7; see details in Table 2).

4.1.3.3.2. Interpretation. The silty to medium-grained sandstone deposits are a product of a suspension process intercalated with bedload transport (Talbot and Allen, 1996; Collinson, 1996; Bridge, 2006; Le Hir et al., 2011), associated with natural levee and crevasse splay deposits on the floodplain (Hughes and Lewin, 1982; Miall, 2000, 2002; Nichols, 2009). When the rupture of marginal levee involves smaller volumes and/or predominance of bedload transport, the overflow forms small shallow channels (lenticular St facies; crevasse-channel) or expands as an unconfined flow (Shf and Srf facies), within the floodplain (Hughes and Lewin, 1982; Miall, 2000; Nichols, 2009).

If the sediment/water mixture acquires density flow characteristics (Sm facies), more continuous beds are formed (DeCelles et al., 1991; Finzel and McCarthy, 2005). The presence of strata without cross-lamination, parallel lamination and climbing ripples, such as massive sandstones beds, are associated with hyperconcentrated density flow. The massive sandstones with scattered granules, small pebbles, and bones are associated with these flows, where shear stress rate is moderate, with friction between grains occurring without collisions (e.

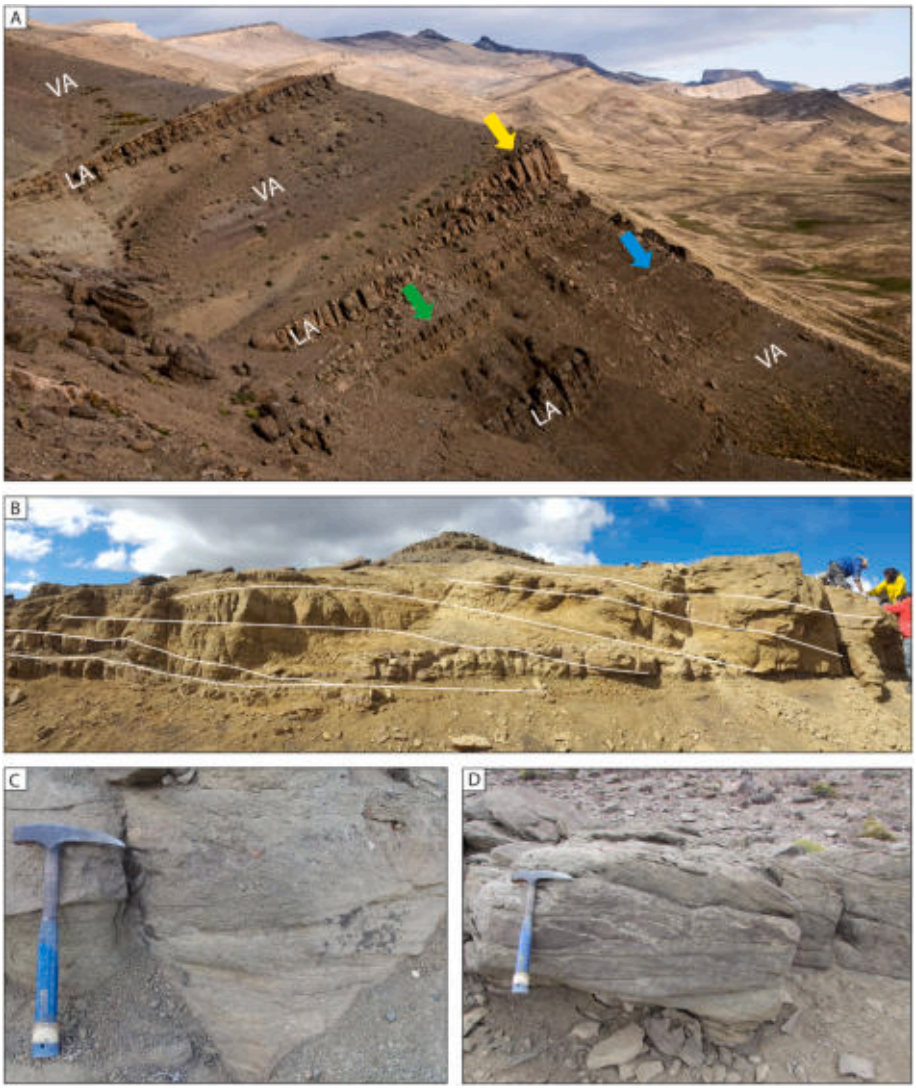

Fig. 5. (A) The larger architectural elements correspond to the laterally continuous flood plain mudstone facies (low relief) and the point bars (lenses that stand out in the topography). The fine-grained sandstone accumulation at the top of the point bar (yellow arrow) corresponds to natural-levee deposits. The thinner lenses of sandstone immersed in mudstone (green arrow) correspond to crevasse-channel deposits, and more continuous and thin sandstone beds (blue arrow) are associated with crevasse splays. Floodplain deposits (vertical accretion) predominate in moments of greater accommodation/sediment supply (A/S) ratio, and with the point bars more widely spaced. The reduction in A/S allows for a greater concentration of sandy deposits as the channels migrate laterally, but without aggradation or with very slow aggradation (Ramón and Cross, 1997). In the channel-belt indicated in the middle part, it is possible to observe the lateral migration with low aggradation. (B) Point bar deposits. The white lines (sigmoidal erosive surfaces) delimit the lateral accretion surfaces. At this level an articulated *Stegouros elengassen* skeleton was found. (C-D) Trough cross-beddings: (C) In the point bar. (D) In the crevasse-channel. Abbreviations: VA: vertical accretion, LA: lateral accretion.

g., Drake, 1990; Mulder and Alexander, 2001). Furthermore, rafting is common in these flows, and can transport large blocks (in this case, a skeleton of an articulated ornithischian, see Table 2) over considerable distances (Mulder and Alexander, 2001).

In turn, layers with diffuse inverse to normal grading (traction carpets; Sohn, 1997) are associated with high shear stress and intense grain collision, grain flow or hyperconcentrated density flow (e.g., Drake, 1990; Mulder and Alexander, 2001). The main mechanism for deposition from these hyperconcentrated density flows is frictional freezing resulting from grain-to-grain interaction (Kneller and Branney, 1995; Lee, 2019).

In the context of fluvial sedimentation, the occurrence of both diffuse lamination and massive sandstones are compatible with the existence of fast and intermittent density flows, triggered by ruptures of marginal levee during intense rainstorms (Mulder and Alexander, 2001).

4.2. *Fossil plant remains in floodplain deposits*

The fossil flora in Fm facies is composed mainly of pteridophyte, pteridosperm, gymnosperm, and angiosperm leaves (sequence 5; see Table 2 for details). Plant macrofossils include leaves, stem fragments and other structures such as reproductive organs (e.g., cones, fruits and seeds). Pteridosperms are abundantly represented by taenopterid-type leaves (Fig. 10A). Gymnosperms show taxonomic affinities with Araucariaceae and Podocarpaceae (Fig. 10B). Angiosperm leaves show affinities with Nothofagaceae and other families like Lauraceae andMalvaceae (Fig. 10C). Towards the top of the succession (Fig. 2), fewer leaf morphotypes have been identified. Leaves found at this facies are highly fragmented and occur associated with abundant plant debris (Fig. 10D). Fern pinnae and angiosperms have been recorded too. Among the angiosperm remains, Nothofagaceae constitutes the most abundant element in this section. In addition, some isolated gymnosperm remains (large-sized leaves and delicate reproductive structures

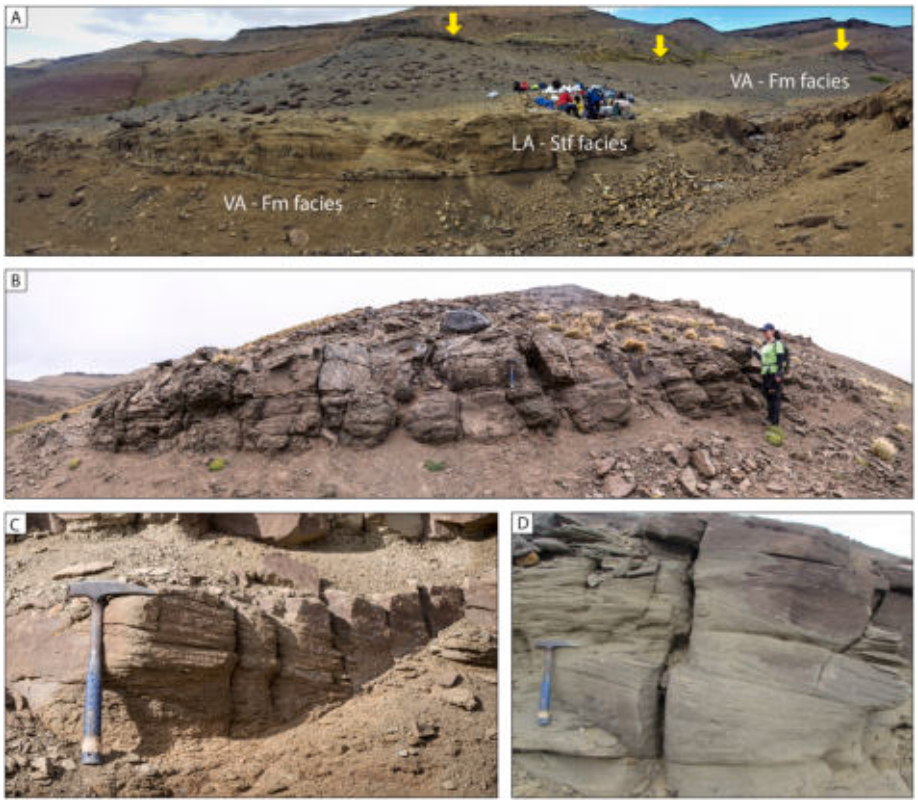

Fig. 6. Point bar facies association. (A) Yellow arrows indicate elongated lenticular beds of sandstone with trough cross-bedding (lateral accretion, St facies), within massive mudstone facies (vertical accretion, Fm facies). (B) Medium-grained sandstone with trough cross-bedding representing a bar-channel deposit. (C) Coarse-grained sandstone with trough cross-bedding. (D) Medium-grained sandstone with trough cross-bedding, where disarticulated sauropod bones were found. Abbreviations: VA: vertical accretion, LA: lateral accretion.

related to Araucariaceae) were also found (Fig. 10E).

In the R facies, abundant fragments of plant impressions and palynological content have been recognized (see Table 2 for details). In the sequence 4, pteridophyte macrofossils are abundant, including the extinct genus *Cladophlebis,* together with representatives of Equisetales and, the Dicksoniaceae and Gleicheniaceae families (Fig. 10F). Aquatic fern roots and rhizomes are very abundant as well as Equisetales ribbed stems. Angiosperms are represented by monocotyledonous leaves (assigned tentatively to Poales cf. Typhaceae, Cúneo et al., 2014; Fig. 10H) and dicotyledonous leaves (Fig. 10G–I). The palynological content (sequence 4, Figs. 2 and 3) associated with the previously mentioned plant macrofossils material is characterized by the high percentage of ferns. The dominant elements correspond to spores with affinities to Cyatheaceae and Gleicheniaceae. In the assemblage there is also pollen attributable to Podocarpaceae, Araucariaceae and Proteaceae (Fig. 11). The taxa *Cyathidites* and *Gleichenidites* are the most abundant miospores, comprising a 40% of the assemblage (Table 1- see supplementary material).

In sequence 5, fossil wood remains and moderate to well-preserved palynomorphs were recovered at a level of hadrosaur bones (Figs. 2, 3 and 7; see Table 2 for details). The palynomorphs in this level are related to gymnosperm families Araucariaceae and Podocarpaceae. Angiosperms related to Arecaceae, Proteaceae and Ericaceae families were identified. In addition, a smaller percentage of spores associated with the Blechnaceae, Gleicheniaceae and Cyatheaceae families are present in this assemblage (Fig. 11). *Araucariacites* and *Arecipites* are the most abundant miospores in this facies, which represents 40% of the assemblage, followed by 23% of Podocarpaceae (Table 1- see supplementary material).

4.3. Shallow marine facies association

4.3.1. Shallow marine facies association

4.3.1.1. Description. These deposits are characterized by medium to coarse-grained sandstones (Stw and Sbio, Table 1, Fig. 12A, B, D) with medium to large-scale trough cross-bedding (0.3 to 1.5 m-thick), ripple cross-lamination, horizontal lamination (Shw, Table 1, Fig. 12B), and mudstones with horizontal lamination (Fh, Table 1). They form lenticular beds with a great lateral extent (more than 5 km), limited by erosive surfaces. The sandstones beds are quartz-rich sandstones, with minor feldspars. These deposits preserve abundant fossils of marine vertebrates and invertebrates, as like as, bivalves, gastropods, shark teeth, plesiosaurs and mosasaurs bones. The bioturbations occur with moderate to low intensity, represented by ichnofabric of *Ophiomorpha*, *Skolithos,* and *Thalassinoides*. Paleocurrent data indicate main sediment transport to the S-SE and subordinately to the N-NE. The grayish purple to gray mudstones preserves osteoderm fragments, shark teeth and plesiosaurs isolated bones.

4.3.1.2. Interpretation. The medium-to coarse grained sandstone and conglomerate deposits are interpreted as a product by combination of unidirectional traction flows (currents) and wave-induced oscillatory flows (Perillo et al., 2014), forming 3D-dunes related to longshore currents in upper shoreface (McCubbin, 1982; Johnson and Baldwin, 1996; Reading and Collinson, 1996). The dominant paleocurrent direction (south-southeast and north-northeast) indicates longshore currents parallel to the coast (Manríquez et al., 2021). The fine sediments are associated with suspension processes (Greenwood and Xu, 2001) in offshore-transition conditions (De Raaf et al., 1977; Greenwood and Xu, 2001). The medium-to coarse grained sandstones with horizontal

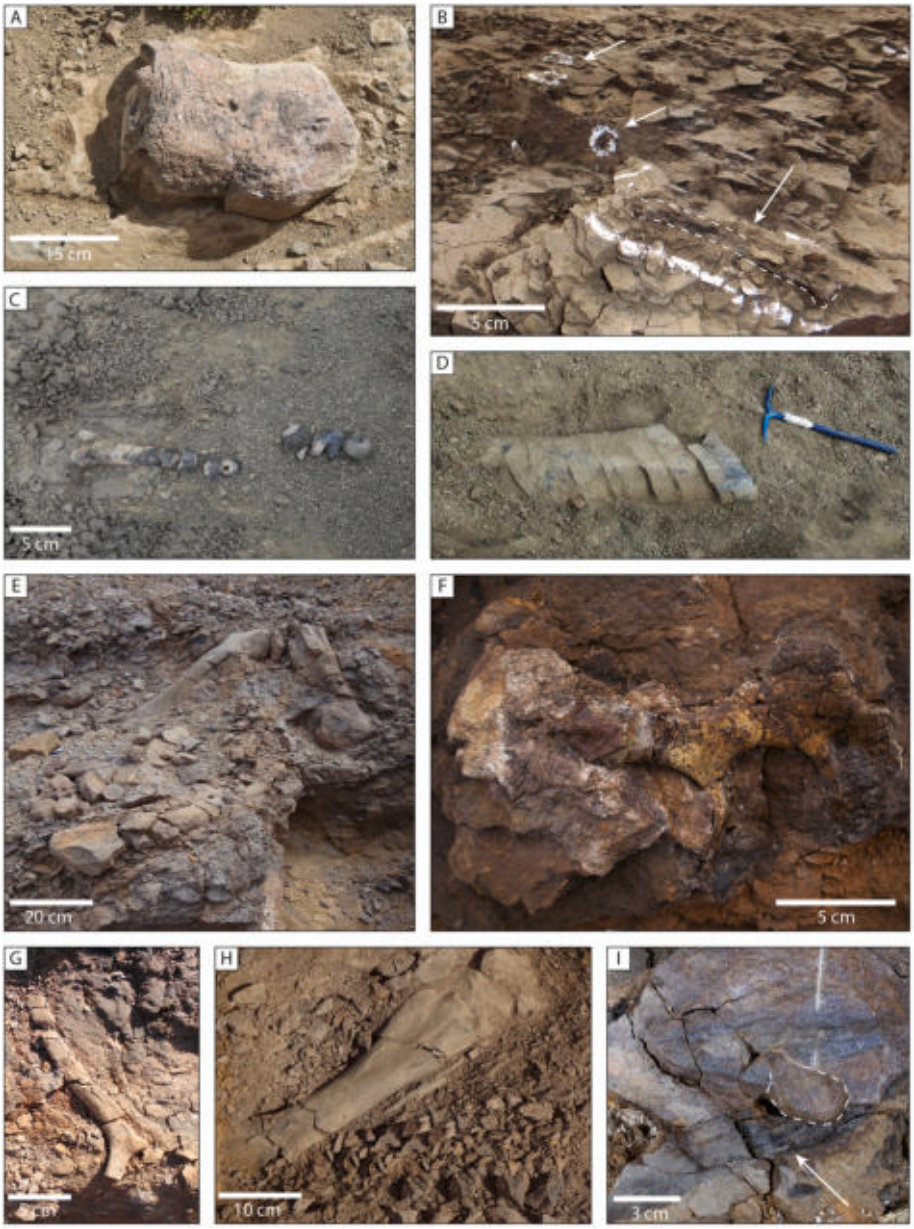

Fig. 7. Vertebrate remains. (A) Caudal vertebra of a sauropod dinosaur preserved in trough cross-bedding sandstone facies. (B) Dispersed bones of small vertebrates preserved in massive sandstone facies. (C) Detail of a long bone and other fragments of small mammals in massive sandstone facies. (D) An incomplete femur of a sauropod dinosaur preserved in massive mudstone facies. (E) Associated long bones of the hadrosaur *Gonkoken nanoi* (femur, tibia, and an incomplete long bone in the foreground) preserved in rhythmite facies. (F) Skull bone of a hadrosaur (*Gonkoken nanoi*). (G) Isolated rib of a hadrosaur (*Gonkoken nanoi*). (H) An incomplete tibia of a hadrosaur (*Gonkoken nanoi*). (I) Plant remains associated with hadrosaur bones.

lamination are interpreted as a product by upper flow regime in foreshore (Van de Meene et al., 1996; Johnson and Baldwin, 1996).

4.3.2. Tidal channel bar facies association

4.3.2.1. Description. These deposits consist principally of moderate-to well-sorted medium scale trough cross-bedding medium-grained sandstones with mud drapes and mud clast on the foresets, and thin beds (<10 cm) of rippled fine-grained sandstones with flaser bedding, forming lenticular beds (Stt and Srt, Table 1, Fig. 12C–E), with at least 5 km of lateral continuity. The bioturbation occurs with moderate intensity, represented by ichnofabric of *Asteriacites*, *Diplocraterion*, *Gyrochorte*, *Lockeia*, *Scolicia, Skolithos,* and *Thalassinoides*. Paleocurrent measurements indicate main sediment transport to the N-NE.

4.3.2.2. Interpretation. Moderate-to well-sorted trough cross-bedding medium-grained sandstones and rippled fine-grained sandstones deposits were developed in a tidal channel (channel bar deposits). The higher ichnodiversity, ichnodisparity, and bioturbation intensity are evidenced by the presence of trace fossils of the archetypal *Cruziana* ichnofacies (e.g., Bromley, 1996; Pemberton et al., 2001; Buatois and Mángano, 2011). These traces are indicative of more stable conditions in the substrate, benthic colonization of less energetic, more ecologically stable substrates, reflecting preferential deposition during fair-weather conditions in the subtidal zone (Bromley, 1996; Pemberton et al., 2001). The dominant paleocurrent direction is parallel to the paleo-coastline (Manríquez et al., 2021). These tidal channel bar deposits represent transitional environments developed at the fluvial–marine interface. Their stratigraphic position, lateral continuity, and paleocurrent patterns parallel to the paleo-coastline indicate

Table 2
Vertebrate and plant fossils record and their taphonomic features.

Depositional sequence	Facies	Fossils
Sequence 3	Gm/ Gt	Scattered wood fossil fragments.
	Stf	Isolated bones of sauropod dinosaurs (vertebrae and fragments of appendicular bones), disarticulated bones of freshwater turtles (cf. *Yaminuechelys* sp.), and isolated bones of frogs. Wood fossil remains. The vertebrate and wood remains present a chaotic orientation and a dispersed distribution.
	Sm/ Shf	Diverse flora characterized by the presence of bryophyte remains (e.g., Marchantiophyta) and a predominance of angiosperms, mainly represented by Nothofagaceae and Lauraceae. Dicotyledonous leaves are generally well preserved and exhibit low fragmentation, commonly displaying up to third- or fourth-order venation. Fern remains are comparatively scarce.
	Fm	Isolated bones of sauropod dinosaurs.
Sequence 4	Stf	A partially articulated skeleton of *Stegouros elengassen* and scattered wood fossil fragments.
	Sm/ Shf	An articulated skeleton of an ornithischian dinosaur and wood fossil fragments. Freshwater turtles (shell and appendicular fragments principally), frogs (mostly appendicular bones), theropods (mainly teeth and fragments of appendicular bones), birds (appendicular bones), teeth of *Magallanodon baikashkenke*, a partial dentary of *Orretherium tzen,* a maxilla fragment of *Yeutherium pressor,* and axial and appendicular bones of indeterminate mammals. The vertebrate remains present a chaotic distribution, scattered and loosely packed.
	Fm	Disarticulated sauropods, anurans and turtle bones. The vertebrate remains present a chaotic orientation and a dispersed distribution.
	R	Abundant pteridophyte fossils are present, including fern pinnae, complete and exceptionally well-preserved fronds, and delicate reproductive structures assignable to *Cladophlebis*, as well as members of Equisetaceae, Dicksoniaceae, and Gleicheniaceae. Aquatic fern roots and rhizomes are also recorded.Angiosperms are represented by broad leaf fragments, occasionally reaching up to 30 cm in length, with a prominent midrib and parallel venation. Dicotyledonous leaves consist of large, complete laminae that are exceptionally well preserved, commonly exhibiting fifth- to sixth-order venation.Associated with these leaf fossils are large stems and portions of tree branches (up to ~25 cm in length), in some cases preserving attached petiolate leaves.
Sequence 5	Fm	Abundant compressions of pteridosperms, particularly pteridosperms leaves, are present. Well-preserved taenopterid leaves, together with Nothofagaceous leaves, constitute the most abundant elements of the assemblage. Pteridophytes (ferns) are represented by frond fragments occurring at multiple stratigraphic levels in varying proportions. Gymnosperms are mainly represented by fragmented leaves and poorly preserved reproductive structures, including members of Podocarpaceae and Araucariaceae. Dicotyledonous leaves are generally well preserved, commonly exhibiting third- to fourth-order venation, and include representatives of Nothofagaceae, Lauraceae and Malvaceae. Fragments of trunks assignable to *Austroginkgoxylon dutrae*, *Agathoxylon antarcticum*, *Podocarpoxylon paradoxi*, *Podocarpoxylon mazzonii*, *Palmoxylon subantarcticae* and *Notomalvaceoxylon magallanense.* are also recorded
	R	Abundant bones of the *Gonkoken nanoi* of different sizes, forming a bonebed. The elements correspond to cranial fragments, appendicular bones, and vertebrae. The bones are disarticulated or semi-articulated. Several bones have a chaotic orientation, although some of them, especially the longest ones, such as humeri, femora and tibiae, tend to be oriented in a north-south direction.
Sequence 6	Fm	Indeterminate plant debris.

increased marine influence during shoreline landward migration. Rather than forming an isolated system, tidal channels are part of an integrated fluvial–coastal continuum controlled by relative sea-level changes.

4.4. Spatial distribution of facies association

The stratigraphic log shows a vertically stacked succession that records the spatial and temporal migration of depositional environments from dominantly fluvial to marginal-marine and shallow-marine settings (Fig. 2). The lower part of the section is characterized by floodplain deposits with fluvial channels (longitudinal bars, point bar and floodplain facies association) represented by mudstones interbedded with sandy to gravelly channel fills and coal-bearing intervals, indicating low-energy overbank environments punctuated by episodic high-energy fluvial discharge. These deposits reflect a laterally extensive alluvial plain with migrating channels.

Up-section, fluvial deposits progressively transition into tidally influenced environments, as indicated by tidal channel bars and mixed fluvial–tidal facies. The presence of heterolithic bedding, wave ripples, and tidal cross-bedding suggests increased marine influence and lateral connectivity with coastal systems. This interval reflects landward migration of shoreline environments during transgressive phases.

The middle to upper part of the succession is dominated by foreshore to upper shoreface deposits, composed mainly of well-sorted sandstones with wave-generated structures, indicating higher-energy shallow-marine conditions. These facies show a basinward shift of depositional environments and record shoreline progradation and retrogradation linked to relative sea-level fluctuations.

Floodplain and upper shoreface deposits alternate in the uppermost part of the section, reflecting repeated shifts between continental and shallow-marine settings. Sequence boundaries and system tracts highlight the spatial reorganization of depositional environments through time, controlled by relative sea-level changes and sediment supply.

5. Discussion

5.1. Paleoenvironmental evolution

The continental/coastal succession exposed in the Río de las Chinas Valley records the evolution of a fluvial system interacting repeatedly with shallow-marine environments (Fig. 13). The dominant depositional setting corresponds to sinuous fluvial channels, represented by fining-upward sandstone bodies with lateral accretion (Stf facies), embedded within an extensive muddy floodplain (Fm facies). Floodplain deposits include crevasse splays (Stf, Shf, Sm, and Srf facies), abandoned channels (R facies), swampy areas, and lagoonal settings, all characterized by an abundant fossil record of plants and vertebrates.

Less frequently, laterally extensive sandy to conglomeratic channel bodies composed of fining-upward Gm, Gt, and Stf facies occur interbedded within floodplain deposits. These bodies reflect higher-energy fluvial conditions and are interpreted as braided-channel fills dominated by longitudinal bar accretion. The vertical and lateral association of these channel types within a predominantly muddy floodplain suggests spatial variability in discharge and sediment supply rather than systematic downstream changes in slope. The close spatial association between deposits interpreted as sinuous channels (characterized by

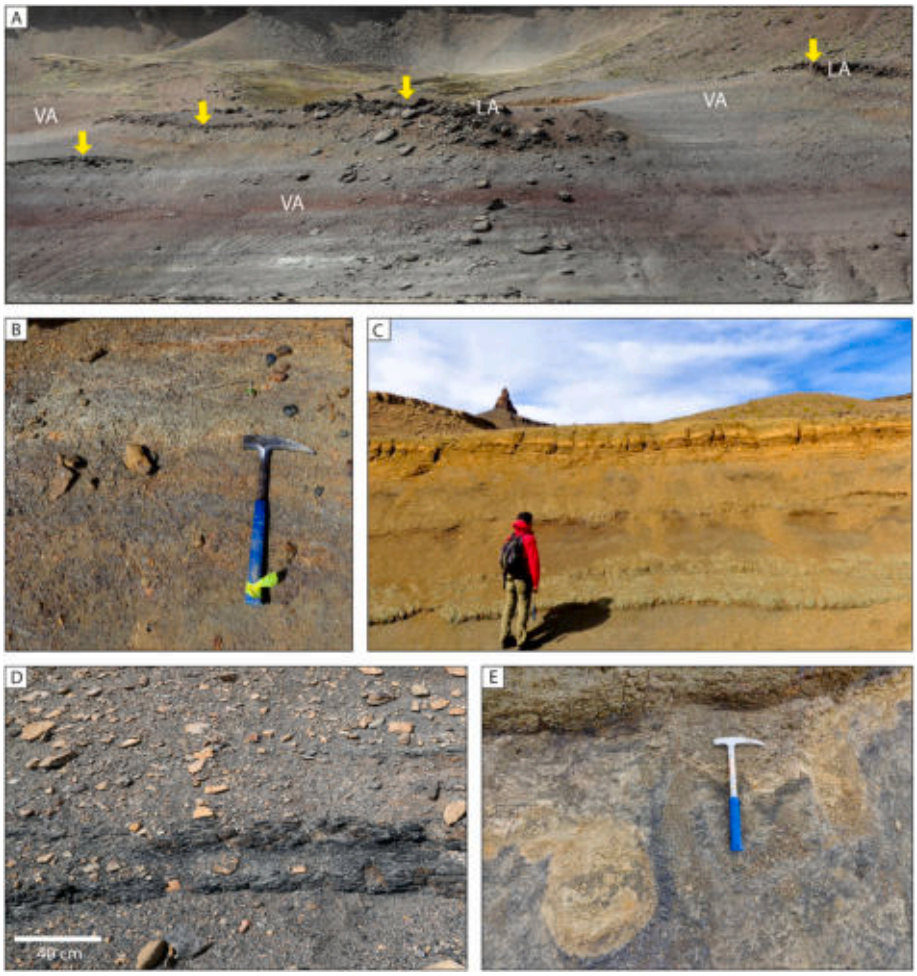

Fig. 8. Floodplain facies association. (A) Massive mudstone level (vertical accretion) with great lateral extension and elongated lenticular beds of sandstones (lateral accretion). (B) Whitish gray mudstones with incipient horizontal lamination, where abundant fragments of plant impressions were found. (C) Rhythmite facies. Intercalation of whitish gray sandy mudstone and claystone, where abundant fragments of plant impressions were found. (D) Elongated lenticular unit of coal with variable thickness (up to 1 m thick by 1 km long). (E) Load cast in mudstone levels. Abbreviations: VA: vertical accretion, LA: lateral accretion.

lateral-accretion deposits) and gravelly channel bodies interpreted as braided reaches suggests that these elements formed within the same fluvial system rather than representing independent drainage networks. At the scale of the studied outcrops, the alternation between these deposits throughout the succession indicates that different channel morphologies likely coexisted within the same fluvial corridor.

The high proportion of mudstone deposits throughout the succession (approximately 70%) suggests deposition in a very low-gradient setting, with slopes estimated between 0.01° and 0.5° (Moscariello, 2018). In such environments, sediment transport is dominated by suspension processes, whereas tractional transport plays a subordinate role. Frequent crevasse-splay deposits and massive sandstones related to hyperconcentrated flows point to episodic, high-magnitude flood events, likely triggered by intense rainfall under humid climatic conditions.

Up-section, fluvial deposits become increasingly interbedded with shallow-marine facies, reflecting direct interaction between continental drainage systems and the coastal realm (Fig. 13). Fluvial channels remain relatively small and do not form well-developed deltas, as sediment was redistributed along a linear, high-energy coastline by strong littoral currents. This coastal plain–shoreface system is characterized by abundant marine invertebrate and vertebrate remains (Soto-Acuña et al., 2016b; Manríquez et al., 2019, 2021; Bravo-Ortiz et al., 2022), and records repeated shoreline shifts controlled by relative sea-level changes.

Overall, the paleoenvironmental evolution is best explained by changes in accommodation linked to relative sea-level fluctuations, which governed the alternation and spatial juxtaposition of fluvial, coastal plain, and shallow-marine environments, rather than by strict adherence to end-member continental fluvial models.

5.1.1. *Channel morphology and sediment supply*

The sedimentary facies architecture demonstrates the coexistence of sinuous channels with point bars, and braided channels with longitudinal bars occurring side by side within the same fluvial system (Fig. 14). This coexistence cannot be satisfactorily explained solely by downstream variations in slope or by base-level position (e.g., braided channels during lowstand and meandering channels during highstand; Nichols, 2009; Catuneanu et al., 2011). Instead, the observed patterns are more consistent with differences in sediment supply and catchment size within the upstream drainage network. Paleocurrent measurements obtained from trough cross-bedding show a dispersed pattern, including north-, northeast-, east-, south-, and southwest-directed sediment transport throughout the succession. Rather than indicating the presence of independent drainage systems, this variability most likely reflects local channel migration and bar accretion processes within a single low-gradient fluvial system. In such settings, paleoflow dispersion commonly results from lateral channel migration, avulsion, and the development of multiple active channels across the floodplain. Consequently, the paleocurrent data are interpreted as representing spatial

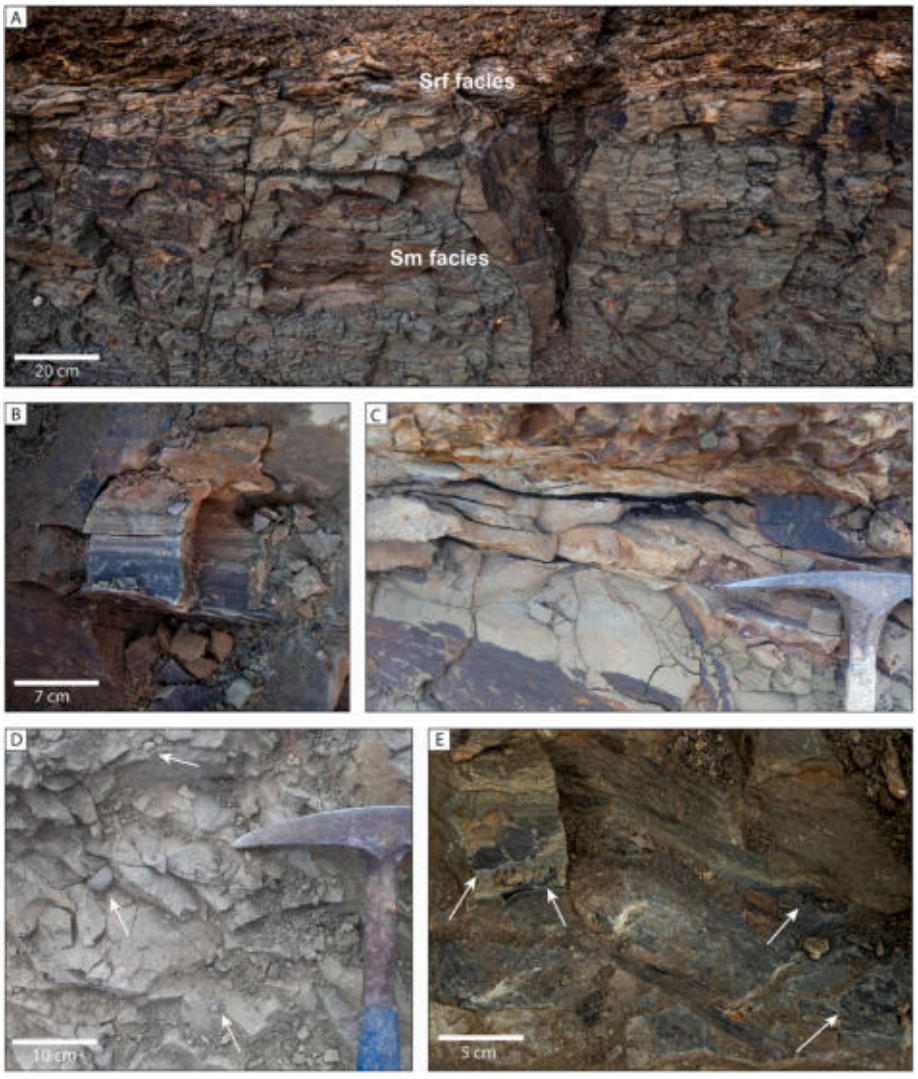

Fig. 9. Crevasse splays facies. (A) Massive sandstone facies (Sm) associated with hyperconcentrated density flow. (B) Sandstone with incipient horizontal lamination (Sh). (C) Sandstone with ripple cross-lamination (Srf) and coal lenses. (D) Massive sandstone facies (Sm). The white arrows show dispersed granules and organic matter. (E) The arrows show some plant impressions in the massive to horizontal lamination sandstone bed (sequence 3).

variability in sediment transport pathways within the same fluvial corridor.

Gravelly channel deposits with longitudinal bars represent reaches characterized by higher bedload input, whereas sandy sinuous channels reflect sectors of the system dominated by suspended load. These channel types were active contemporaneously and fed the same coastal system, highlighting spatial heterogeneity within the fluvial domain. Importantly, their development took place under similar climatic conditions and within a depositional framework repeatedly influenced by marine transgressions and regressions.

The dominance of floodplain deposits, the lateral coexistence of different channel morphologies, and the recurrent interfingering of fluvial and marine facies indicate a low-gradient coastal plain where fluvial architecture was strongly modulated by accommodation changes driven by relative sea-level fluctuations. In this context, braided and sinuous channels reflect variable sediment supply from distinct upstream sectors rather than discrete zones of a radial fluvial system.

Our fluvial system (Fig. 13) was developed in a warm and humid climate from the late Campanian to the early Maastrichtian, becoming a slightly colder and drier towards the late Maastrichtian. These observations are supported by previous paleoclimatic studies based on dicot leaf physiognomy (Pino et al., 2016; Leppe et al., 2017). Microthermal conditions (cool mean annual temperatures) and high seasonal variation in temperatures and precipitations are discussed in detail in the next item.

The stratigraphic distribution of channel deposits also suggests that relative sea-level variations played an important role in controlling fluvial style. As illustrated in Fig. 3, deposits interpreted as frontal or longitudinal bars tend to occur preferentially toward the upper parts of the depositional sequences. This vertical distribution is consistent with an intrinsic shallowing trend and reflects decreasing accommodation during the late stages of sequence development. Under these conditions, channel deposits become increasingly amalgamated and higher-energy bar forms are preferentially preserved. Increased sediment supply relative to accommodation likely favored the development of braided channel reaches. Consequently, the sedimentary record is interpreted as representing a single fluvial system whose internal morphology and depositional style were strongly modulated by variations in sediment supply and accommodation linked to relative sea-level fluctuations.

5.2. *Environmental and climatic implications of fossil records*

The vegetation communities within the floodplain facies association were dominated by gymnosperms and angiosperms. Numerous leaf

Fig. 10. Plant fossil outcrops at mudstone facies (El Puesto locality): (A) Very well-preserved venation of a taenopterid leaves. (B) Small size leaves of gymnosperm material. (C) Well-preserved, partly incomplete dicot leaves. (D) Highly fragmented fossil leaves with abundant plant debris. (E) Fragmented Nothofagaceous leaves. Plant fossil outcrops at rhythmite facies ("Saurópodo" locality). (F) Sterile and reproductive fern fronds. White arrows indicate delicate reproductive structures. (G) Very well-preserved large dicot leaf of indeterminate affinity with visible areolation. (H)A large monocot leaf assignable to cf. Typhaceae. White arrows indicate the wide leaf midrib. (I) Portion of a tree branch bearing an attached angiosperm leaf.

fragments display expanded petiole bases that are consistent with natural abscission and the development of seasonal litter inputs (Meldahl et al., 1995; Thomas et al., 1999; Taylor and Whitelaw, 2001). However, deciduousness should be treated as a working hypothesis and evaluated alongside independent proxies for seasonality and hydrologic stress, such as paleopedological indicators of rainfall seasonality (Raigemborn et al., 2025).

Fern fronds occur throughout the floodplain deposits, generally with low diversity, specifically in the massive mudstone beds of the base of sequence 5 (Fig. 2). In sequence 5, high abundance, good preservation, and low degree of fragmentation of *Nothofagus* and taenopterid leaves (Fig. 2), are consistent with an autochthonous to parautochthonous signal, implying deposition close to the source vegetation (Greenwood, 1991; Gastaldo, 2001). This interpretation is compatible with palynological evidence from correlative late Maastrichtian floodplain successions in southern Patagonia, where the presence of abundant spores and pollen massulae has been interpreted as reflecting short transport and deposition near the parental vegetation (Novas et al., 2019; Vera et al., 2022; Moyano-Paz et al., 2022; Loinaze et al., 2025).

In contrast, the occurrence of relatively complete leaves attributable to Araucariaceae and Podocarpaceae may reflect either (i) selective preservation during transport due to coriaceous leaf textures, and/or (ii) contributions from better-drained sectors of the floodplain or extrabasinal areas. Rather than relying on modern ecological co-occurrence

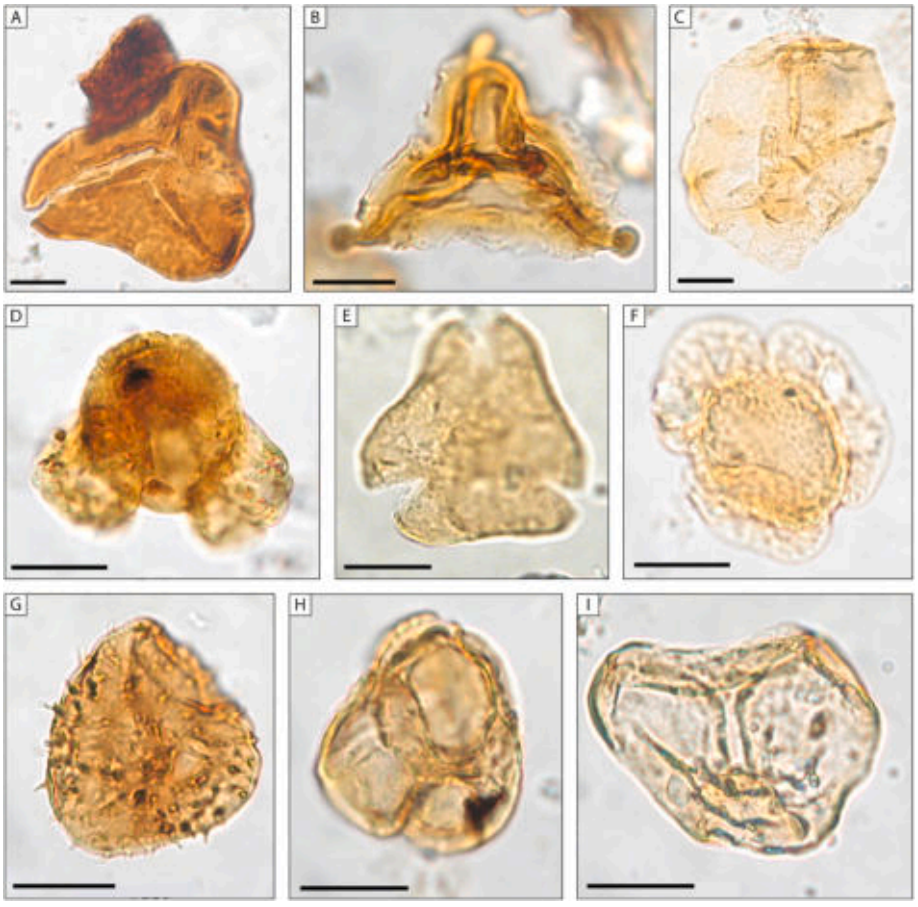

Fig. 11. Palynological record of the Rhythmite facies. (A) *Cyathidites* sp. (B) *Clavifera triplex* (Gleicheniaceae). (C) *Microcachridites* sp. (Podocarpaceae). (D) *Podocarpidites otagoensis* (Podocarpaceae). (E) *Peninsulapollis gillii* (Proteaceae). (F) *Dacrycarpites australiensis* (Podocarpaceae). (G) *Spinizonocolpites* sp. (Arecaceae). (H) *Ericipites* sp. (Ericaceae). (I) *Trichotomosulcites* sp. (Podocarpaceae). Scale: 10 μm.

as a transport proxy, the allochthonous component should be evaluated with explicit taphonomic criteria (sorting, orientation, fragmentation spectra, and association with plant debris) and facies context.

Towards the top of the succession (sequence 6), highly fragmented leaves with moderate preservation and dispersed plant debris across beds suggest increased reworking and longer transport distances, supporting a more allochthonous signal for the assemblage (Greenwood, 1991; Gastaldo, 2001). Associated to R facies in sequence 4, the high degree of preservation, completeness of fossil leaves and the size of plants remains, suggest little transport before the deposition of the material, indicating an autochthonous to parautochthonous origin of the flora (Greenwood, 1991; Gastaldo, 2001). The presence of Equisetales, aquatic ferns (Marsileaceae), and Typhaceae leaves is also consistent with riparian vegetation deposited in shallow, low-energy waters. Gray lithologies, commonly associated with organic matter accumulation and reducing conditions, together with the occurrence of rhizoliths, further support humid conditions with localized soil development (Retallack, 2001; Retallack, 2001).

From a palynological perspective, climatic interpretations of the Río de las Chinas succession should distinguish between basin-scale climate signals and local hydrologic controls operating within the floodplain. In the R facies at the base of the succession (Sequence 4; Fig. 2), the dominance of *Cyathidites* and *Gleichenidites* indicates hygro-mesophytic conditions (Wang et al., 2005; Bowman et al., 2014), consistent with warm and humid environments during the late Campanian–early Maastrichtian. Assemblages from Sequence 5 (late Maastrichtian) show increased proportions of *Araucariacites* and *Arecipites*, taxa commonly associated with thermo-xerophytic or subtropical affinities. However, recent quantitative palynological studies of the upper Maastrichtian Chorrillo Formation document only moderate changes in taxon proportions without major floristic turnover, suggesting subtle variations in humidity regime and/or habitat partitioning rather than a pronounced climatic shift (Loinaze et al., 2025).

Paleosol-based climofunctions independently constrain late Maastrichtian climate in southern Patagonia as temperate to humid subtropical, characterized by marked rainfall seasonality and only minor fluctuations (Raigemborn et al., 2025). Accordingly, differences observed between stratigraphic intervals are more parsimoniously interpreted as reflecting variations in rainfall seasonality and floodplain drainage conditions, superimposed on an overall humid temperate to warm climatic background.

6. Conclusion

The Río de las Chinas Valley succession records the development of a fluvial system in a high-latitude foreland basin during the end of the Cretaceous, characterized by repeated interaction between continental and shallow-marine environments. Sedimentological and paleontological data indicate deposition within a low-gradient fluvial plain connected to a high-energy, linear coastline. Fluvial architecture is defined by the lateral coexistence of sinuous channels and gravelly channel reaches characterized by longitudinal bars within an extensive muddy floodplain. This configuration reflects spatial variability in sediment supply and catchment size, with gravel-rich braided channels linked to higher bedload input and sandy sinuous channels associated with reduced sediment availability and dominance of suspended load. Floodplain deposits record frequent overbank flooding, crevasse-splay activity, abandoned channels, and swampy environments, highlighting

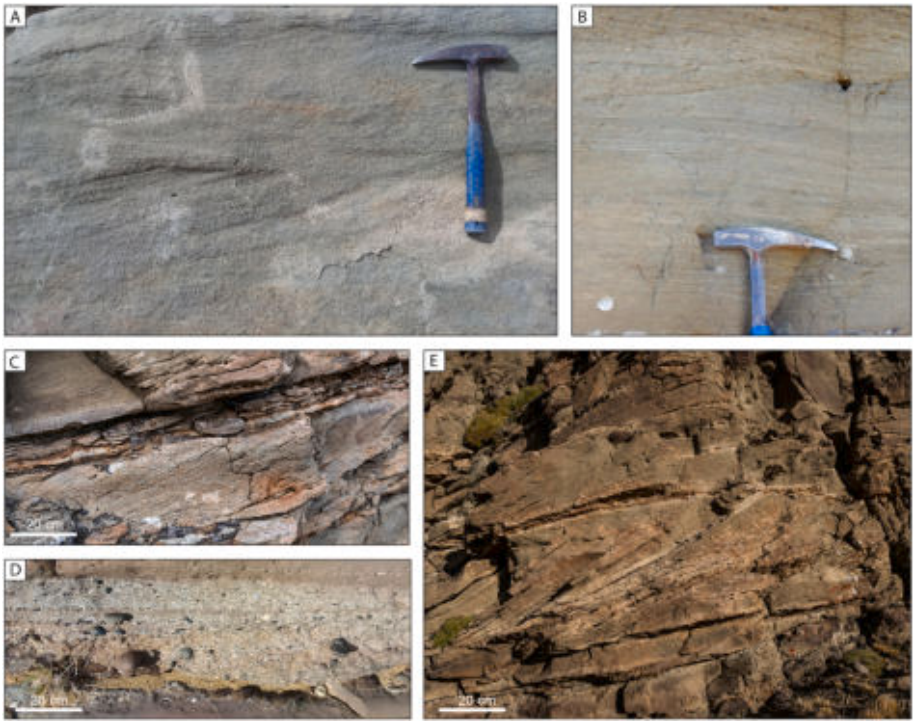

Fig. 12. Marine facies association. (A) Medium-grained sandstones with trough cross-bedding associated to upper shoreface deposits. (B) Medium-grained sandstones with horizontal lamination associated to foreshore deposits. (C) Rippled fine-grained sandstones forming lenticular beds (Srt facies). (D) Medium to coarse-grained sandstones with abundant marine fossils (Sbio facies). (E) Moderate-to well-sorted trough cross-bedding medium-grained sandstones associated to tidal-channel bars.

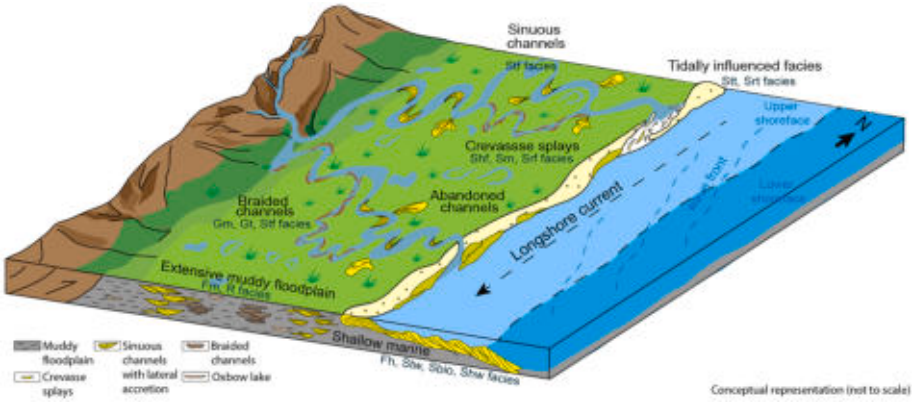

Fig. 13. Conceptual three-dimensional depositional model showing the spatial relationships between fluvial, coastal-plain, and shallow-marine environments in the Río de las Chinas Valley. The model illustrates the coexistence of sinuous channels with lateral accretion deposits (Stf facies) and gravelly, higher-energy braided reaches (Gm, Gt, Stf facies) within a single fluvial system. These channel styles developed under variable discharge and sediment-supply conditions within the same fluvial corridor. Floodplain deposits (Fm, R facies) include crevasse splays (Shf, Sm, Srf facies) and abandoned channels. Basinward, the system transitions into tidally influenced and shallow-marine environments. The block diagram also illustrates the internal sedimentary architecture of the main depositional elements (not to scale).

the importance of accommodation and episodic high-magnitude flood events.

Macrofossil taphonomy and palynology indicate mixed transport signals within the floodplain, controlled primarily by local hydrologic and geomorphic factors rather than by vegetation type alone. Paleobotanical data support warm and humid conditions during the early Maastrichtian, followed by moderate cooling and drying toward the late Maastrichtian. Regional proxy constraints suggest that these changes reflect modest variations in moisture balance and habitat distribution within a persistently humid fluvial landscape at high latitudes during the latest Cretaceous. Overall, these results refine our understanding of fluvial dynamics and climate evolution in high-latitude foreland basins during the latest Cretaceous.

CRediT authorship contribution statement

Leslie M.E. Manríquez: Writing – review & editing, Writing – original draft, Resources, Methodology, Investigation, Formal analysis, Conceptualization. **Ernesto L.C. Lavina:** Writing – review & editing, Resources, Methodology, Conceptualization. **Juan Pablo Pino:** Writing – review & editing, Writing – original draft, Validation, Investigation, Formal analysis. **Cristine Trevisan:** Writing – review & editing, Writing

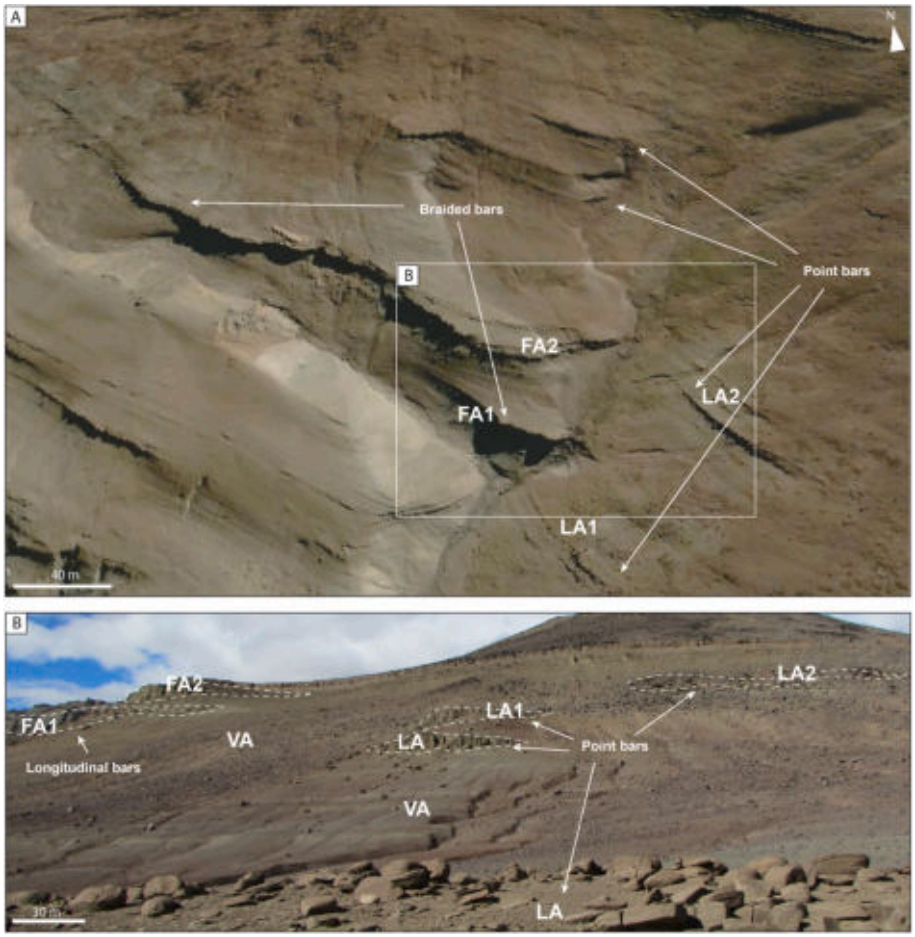

Fig. 14. (A) Oblique aerial view of the studied outcrop showing the spatial association between different bar architectures within the fluvial succession. Gravelly channel bodies characterized by longitudinal bars (FA1–FA2) and lateral-accretion elements (LA1–LA2), typical of sinuous channels, occur within the same fluvial corridor and are laterally juxtaposed at scales of tens of meters. Apparent vertical relationships observed in the image reflect exposure geometry, differential erosion, and oblique viewing angle, and do not represent a simple stratigraphic superposition. (B) Ground-based photograph of the same area highlighting longitudinal-bar, point-bar deposits, valley-axis (VA) zones, and lateral-accretion elements (LA). The close spatial association of these deposits is interpreted as reflecting the coexistence of different channel styles within a single fluvial system, likely controlled by spatial and temporal variations in discharge, sediment supply, and accommodation. Abbreviations: VA: vertical accretion; LA: lateral accretion; FA: frontal accretion.

– original draft, Validation, Investigation, Formal analysis. **Jhonatan Alarcón-Muñoz:** Writing – review & editing, Writing – original draft, Validation, Investigation, Formal analysis. **Joseline Manfroi:** Writing – review & editing, Writing – original draft, Validation, Investigation. **Hector Mansilla:** Validation, Investigation, Formal analysis. **Marcelo Leppe:** Writing – review & editing, Investigation, Formal analysis.

Declaration of competing interest

The authors declare that they have no known competing financial interests or personal relationships that could have appeared to influence the work reported in this paper.

Acknowledgments

We give special thanks to E. González, H. Ortiz, A. Manríquez, V. Milla, V. Lobos, J. Kaluza, F. Suazo, M. Ortuya, S. Garrido, and P. Vargas for their assistance in the field; R. Fernández and E. Guareschi for their valuable assistance in the field and their feedback on the manuscript; A. Martinelli and G. Aguirrezabala for their valuable comments about the vertebrate fossils; R. Quinán for his collaboration with some photographs; J. Cagliari, Schmidt and H. Kern for the text review and criticism. We also give thanks to the Itt Oceaneon of Unisinos University for the laboratory facilities. We also thank the Chilean Antarctic Institute (INACH) for their support during field work. The present study is part of the project "Integrated study of the K-Pg boundary in the Antarctic Peninsula (Seymour Island-Vega Island) and the Magallanes Basin (Río de las Chinas Valley)" (Agencia Nacional de Investigación y Desarrollo de Chile -ANID, Fondecyt Postdoctoral project N° 3230319), and received support for field trips from the Anillo Project (ACT-172099), EVOTEM Millennium Nucleus ANID-MILENIO-NCN2023_025 and Estancia Cerro Guido. J.A.M. and J.P.P are supported by the ANID scholarship for PhD studies in Chile. ELCL and JM thank the Brazilian Council for Research and Technological Development (CNPq) for research grant 310454/2019-0 and 203277/2020-1. Additionally, we extend our thanks to the anonymous reviewer and Marina Coronel for their insightful comments during the review process of this manuscript.

Appendix A. Supplementary data

Supplementary data to this article can be found online at https://doi.org/10.1016/j.eve.2026.100124.

Data availability

No data was used for the research described in the article.

References

Ainsworth, R.B., Vakarelov, B.K., Nanson, R.A., 2011. Dynamic spatial and temporal prediction of changes in depositional processes on clastic shorelines: toward improved subsurface uncertainty reduction and management. AAPG (Am. Assoc. Pet. Geol.) Bull. 95, 267–297.

Alarcón-Muñoz, J., Soto-Acuña, S., Manríquez, L.M.E., Fernández, R.A., Bajor, D., Guevara, J.P., Suazo, F., Leppe, M., Vargas, A.O., 2020. Freshwater turtles (Testudines: Pleurodira) in the Upper Cretaceous of Chilean Patagonia. J. South Am. Earth Sci. 102, 102652. https://doi.org/10.1016/j.jsames.2020.102652.

Alarcón-Muñoz, J., Vargas, A.O., Püschel, H.P., Soto-Acuña, S., Manríquez, L., Leppe, M., Kaluza, J., Milla, V., Gutstein, C.S., Palma-Liberona, J., Stinnesbeck, W., Frey, E., Pino, J.P., Bajor, D., Núñez, E., Ortiz, H., Rubilar-Rogers, D., Cruzado-Caballero, P., 2023. Relict duck-billed dinosaurs survived into the last age of the dinosaurs in subantarctic Chile. Sci. Adv. 9 (24) eadg2456.

Amudeo-Plaza, J., Soto-Acuña, S., Fernández, R., Vargas, A.O., Leppe, M., 2022. Diversidad dental en Ankylosauria (Thyreophora: Ankylosauria) del extremo sur de Sudamérica. Abstracts, II Congreso Chileno de Paleontología. San Vicente de Tagua Tagua 116.

Arbe, H.A., Hechem, J.J., 1984. Estratigrafía y facies de depósitos marinos profundos del Cretácico Superior, Lago Argentino, Provincia de Santa Cruz. Actas IX Congreso Geológico Argentino 5, 7–41.

Ashmore, P.E., 1991. How do gravel-bed rivers braid? Can. J. Earth Sci. 28 (3), 326–341.

Atisha-González, A., Soto-Acuña, S., Amudeo-Plaza, J., Aravena, B., Alarcón, J., Vargas, A.O., Leppe, M., 2022. Nuevo registro de titanosaurios (Dinosauria: Sauropoda) procedentes del Cretácico Superior de la Patagonia chilena. Abstracts, II Congreso Chileno de Paleontología. San Vicente de Tagua Tagua 122.

Auchter, N.C., Romans, B.W., Hubbard, S.M., 2016. Influence of Deposit Architecture on Intrastratal Deformation, Slope Deposits of Tres Pasos Formation, vol. 341. Sedimentary Geology, Chile, pp. 13–26.

Biddle, K.T., Uliana, M.A., Mitchum Jr., R.M., Fitzgerald, M.G., Wrighr, R.C., 1986. The stratigraphic and structural evolution of the central and eastern Magallanes Basin, southern South America. In: Allen, P.A., Homewood, P. (Eds.), Foreland Basins, vol. 8. Special Publication of the International Association of Sedimentologists, pp. 41–61.

Boggs Jr., S., 2006. Principles of Sedimentology and Stratigraphy. Pearson Education, p. 662.

Boyd, R., Dalrymple, R., Zaitlin, B.A., 1992. Clasification of clastic coastal depositional environments. Sediment. Geol. 80, 139–150.

Bowman, V.C., Francis, J.E., Askin, R.A., Riding, J.B., Swindles, G.T., 2014. Latest cretaceous–earliest Paleogene vegetation and climate change at the high southern latitudes: palynological evidence from Seymour Island, Antarctic Peninsula. Palaeogeogr. Palaeoclimatol. Palaeoecol. 408, 26–47.

Bravo-Ortiz, C., Alarcón-Muñoz, J., Bajor, D., Manríquez, L., Cruzado-Caballero, P., Vargas, A.O., Soto-Acuña, S., Leppe, M., 2022. Descripción de fragmentos craneales de un cf. Hadrosauroidea (Ornithopoda: Hadrosauridae) en el Valle del Río de Las Chinas, Región de Magallanes. Abstracts, II Congreso Chileno de Paleontología. San Vicente de Tagua Tagua 123.

Bridge, J.S., 2006. Fluvial Facies Models: Recent Developments, vol. 84. Special Publication-SEPM, pp. 85–170.

Bromley, R.G., 1996. Trace Fossils: Biology, Taphonomy and Applications. Chapman & Hall, London, p. 361.

Buatois, L.A., Mángano, M.G., 2011. Ichnology: Organism-Substrate Interactions in Space and Time. Cambridge University Press, Cambridge, p. 358.

Camacho, H.H., Chiesa, J.O., Parma, S.G., Reichler, V., 2000. Invertebrados Marinos De La Formación Man Aike (Eoceno Medio), Provincia De Santa Cruz, Argentina, vol. 64. Boletín de la Academia Nacional de Ciencias, pp. 187–208.

Catuneanu, O., Galloway, W.E., Kendall, C.G.S.C., Miall, A.D., Posamentier, H.W., Strasser, A., Tucker, M.E., 2011. Sequence stratigraphy: methodology and nomenclature. Newslett. Stratigr. 44 (3), 173–245.

Catuneanu, O., Abreu, V., Bhattacharya, J.P., Blum, M.D., Dalrymple, R.W., Eriksson, P. G., Fielding, C.R., Fisher, W.L., Galloway, W.E., Gibling, M.R., Giles, K.A., Holbrook, J.M., Jordan, R., Kendall, C.G.S.T.C., Macurda, B., Matinsen, O.J., Miall, A.D., Neal, J.E., Nummedal, D., Pomar, L., Posamentier, H.W., Pratt, B.R., Sarg, J.F., Shanley, K.W., Steel, R.J., Strasser, A., Tucker, M.E., Wink, C., 2009. Towards the standardization of sequence stratigraphy. Earth Sci. Rev. 92 (1), 1–33.

Chimento, N.R., Agnolin, F.L., Tsuihiji, T., Manabe, M., Novas, F.E., 2020. New record of a Mesozoic gondwanatherian mammaliaform from Southern Patagonia. Sci. Nat. 107 (6), 1–7.

Cohen, A.D., 1984. The Okefenokee Swamp: Its natural history, geology, and geochemistry. Wetlands Surveys.

Collinson, J.D., 1996. Alluvial sediments. In: Reading, H.G. (Ed.), Sedimentary Environments: Processes, Facies and Stratigraphy. Blackwell Science Ltd., Oxford, pp. 37–82.

Condie, K., 2016. Tectonic setting. In: press, Academic (Ed.), Earth as an Evolving Planetary System. Third Edition, pp. 43–88.

Cortés, R., 1964. Informe Geológico del área Río Las Chinas–Río Bandurrias (Última Esperanza). Empresa Nacional del Petróleo, Magallanes, Punta Arenas, Chile 33.

Covault, J.A., Romans, B.W., Graham, S.A., 2009. Outcrop expression of a continental-margin-scale shelf-edge delta from the Cretaceous Magallanes Basin, Chile. J. Sediment. Res. 79 (7), 523–539.

Cúneo, N.R., Gandolfo, M.A., Zamaloa, M.C., Hermsen, E., 2014. Late Cretaceous aquatic plant world in Patagonia, Argentina. PLoS One 9 (8), e104749. https://doi.org/10.1371/journal.pone.0104749.

Cuitiño, J.I., Varela, A.N., Ghiglione, M.C., Richiano, S., Poiré, D.G., 2019. The Austral-Magallanes Basin (southern Patagonia): a synthesis of its stratigraphy and evolution. Lat. Am. J. Sedimentol. Basin Anal. 26 (2), 155–166.

Dalrymple, R.W., Choi, K., 2007. Morphologic and facies trends through the fluvial–marine transition in tide-dominated depositional systems: a schematic framework for environmental and sequence-stratigraphic interpretation. Earth Sci. Rev. 81, 135–174.

Dalrymple, R.W., Zaitlin, B.A., Boyd, R., 1992. Estuarine facies models: conceptual basis and stratigraphic implications. J. Sediment. Petrol. 62, 147–173.

Dasgupta, S., Ghosh, P., Gierlowski-Kordesch, E.H., 2017. A discontinuous ephemeral stream transporting mud aggregates in a continental rift basin: the Late Triassic Maleri Formation, India. J. Sediment. Res. 87 (8), 838–865.

Davis, S.N., Soto-Acuña, S., Fernández, R.A., Amudeo-Plaza, J., Leppe, M.A., Rubilar-Rogers, D., Vargas, A.O., Clarke, J.A., 2023. New records of Theropoda from a Late Cretaceous (Campanian–Maastrichtian) locality in the Magallanes-Austral Basin, Patagonia, and insights into end Cretaceous theropod diversity. J. South Am. Earth Sci. 122, 104163.

De Raaf, J.F.M., Boersma, J.R., Van Gelder, A., 1977. Wave-generated structures and sequences from a shallow marine succession. Lower Carboniferous, County Cork, Ireland. Sedimentology 4, 1–52.

De Raaf, Boersma, J.R., Van Gelder, S., 1977. Wave-generated structures and sequences from a shallow marine succession, Lower Carboniferous, County Cork, Ireland. Sedimentology 24 (4), 451–483.

DeCelles, P.G., 2012. Foreland basin systems revisited: variations in response to tectonic settings. In: Busby, C., Pérez, A.A. (Eds.), Foreland Basin Tectonics of Sedimentary Basins: Recent Advances. Blackwell Publishing, pp. 405–427.

DeCelles, P.G., Gray, M.B., Ridgway, K.D., Cole, R.B., Pivnik, D.A., Pequera, N., Srivastava, P., 1991. Controls on synorogenic alluvial-fan architecture, Beartooth Conglomerate (Paleocene), Wyoming and Montana. Sedimentology 38, 567–590.

De Mowbray, T., Visser, M.J., 1984. Reactivation surfaces in subtidal channel deposits, Oosterschelde, Southwest Netherlands. J. Sediment. Res. 54, 811–824.

Drake, T.G., 1990. Structural features in granular flows. J. Geophys. Res. Solid Earth 95 (B6), 8681–8696.

Durkin, P.R., Hubbard, S.M., Holbrook, J., Weleschuk, Z., Nesbit, P., Hugenholtz, C., Lyons, T., Smith, D.G., 2020. Recognizing the product of concave-bank sedimentary processes in fluvial meander-belt strata. Sedimentology 67 (6), 2819–2849.

Eberth, D.A., Miall, A.D., 1991. Stratigraphy and evolution of a vertebrate-bearing, braided to anastomosed fluvial system, Cutler Formation (Permian-Pennsylvanian), north-central New Mexico. Sediment. Geol. 72, 225–252.

Fildani, A., Cope, T.D., Graham, S.A., Wooden, J.L., 2003. Initiation of the Magallanes foreland basin: timing of the southernmost Patagonian Andes orogeny revised by detrital zircon provenance analysis. Geology 3, 1081–1084.

Finzel, E.S., McCarthy, P.J., 2005. Architectural Analysis of Fluvial Conglomerate in the Nanushuk Formation, Brooks Range Foothills, Alaska. Division of Geological & Geophysical Surveys, p. 20.

Fosdick, J.C., Romans, B.W., Fildani, A., Bernhardt, A., Calderón, M., Graham, S.A., 2011. Kinematic evolution of the Patagonian retroarc fold-and-thrust belt and Magallanes foreland basin, Chile and Argentina, 51°30'S. Geol. Soc. Am. Bull 123, 1679–1698.

Fosdick, J.C., VanderLeest, R.A., Bostelmann, J.E., Leonard, J.S., Ugalde, R., Oyarzún, J. L., Griffin, M., 2020. Revised timing of Cenozoic Atlantic incursions and changing hinterland sediment sources during southern Patagonian orogenesis. Lithosphere, 8883099. https://doi.org/10.2113/2020/8883099.

Galloway, W.E., 1975. Process framework for describing the morpholofic and stratigraphic evolution of deltaic depositional system. In: Broussard, M.L. (Ed.), Deltas, Models for Exploration. Houston Geological Society, pp. 87–98.

Gastaldo, R., 2001. Plant taphonomy. In: Briggs, D.E.G., Crowther, P.R. (Eds.), Palaeobiology II. Blackwell Scientific, Oxford, UK, pp. 314–317.

George, S.W., Davis, S.N., Fernández, R.A., Manríquez, L.M., Leppe, M.A., Horton, B.K., Clarke, J.A., 2020. Chronology of deposition and unconformity development across the Cretaceous–Paleogene boundary, Magallanes-Austral Basin, Patagonian andes. J. South Am. Earth Sci. 97, 102237. https://doi.org/10.1016/j.jsames.2019.102237.

Ghiglione, M.C., Suarez, F., Ambrosio, A., Da Poian, G., Cristallini, E.O., Pizzio, M.F., Reinoso, R.M., 2009. Structure and evolution of the Austral Basin fold-thrust belt, southern Patagonian Andes. Rev. Asoc. Geol. Argent. 65 (1), 215–226.

Gleason, P. J., Stone, P., 1994. Age, origin, and landscape evolution of the Everglades peatland. Everglades: the ecosystem and its restoration, 149-197.

Goin, F., Martinelli, A., Soto-Acuña, S., Vieytes, E., Manríquez, L., Fernández, R., Pino, J. P., Trevisan, C., Kaluza, J., Reguero, M., Leppe, M., Ortiz, H., Rubilar-Rogers, D., Vargas, A., 2020. First Mesozoic Mammal from Chile: the Southernmost record of Late Cretaceous Gondwanatherian. Boletín del Museo de Historia Natural, Chile 69 (1), 5–31.

Greenwood, D., 1991. The taphonomy of plant macrofossils. In: Donovan, S.K. (Ed.), The Processes of Fossilization. Belhaven Press, London, p. 303.

Greenwood, B., Xu, Z., 2001. Size fractionation by suspension transport: a large scale flume experiment with shoaling waves. Mar. Geol. 176 (1-4), 157–174.

Gutiérrez, N.M., Le Roux, J.P., Vásquez, A., Carreño, C., Pedroza, V., Araos, J., Oyarzún, J.L., Pino, J.P., Rivera, H.A., Hinojosa, L.F., 2017. Tectonic events reflected by palaeocurrents, zircon geochronology, and palaeobotany in the Sierra Baguales of Chilean Patagonia. Tectonophysics 695, 76–99.

Harambour, S., Soffia, J.M., 1988. Transición De Margen Pasivo a Cuenca De Antepaís: Síntesis Evolutiva Para El Extremo Norte De Ultima Esperanza, Magallanes, Chile. V Congreso Geológico Chileno, pp. A385–A402.

Harms, J.C., Southard, J.B., Walker, R.G., 1982. Structures and sequences in clastic rocks. Lecture notes for short course, Soc. Econ. Paleont. Min. 9, 250.

Horton, B.K., 2018. Sedimentary record of Andean mountain building. Earth Sci. Rev. 178, 279–309.
Hubbard, S.M., Fildani, A., Romans, B.W., Covault, J.A., Mchargue, T.R., 2010. High-relief slope clinoform development: insights from outcrop, Magallanes Basin, Chile. J. Sediment. Res. 80, 357–375.
Hughes, D.A., Lewin, J., 1982. A small-scale flood plain. Sedimentology 29 (6), 891–895.
Jones, T.P., Rowe, N.P., 1999. Fossil Plants and Spores: Modern Technics. The Geological Society, Londres, p. 396.
Johnson, H.D., Baldwin, C.T., 1996. Shallow marine seas. In: Reading, H.G. (Ed.), Sedimentary Environment: Processes. Facies and Stratigraphy. Blackwell Publishing, Oxford, pp. 232–280.
Katz, H.R., 1963. Revision of Cretaceous Stratigraphy in Patagonian Cordillera of Última Esperanza, Magallanes Province, Chile, vol. 47. American Association of Petroleum Geologist Bulletin, pp. 506–524.
Klein, G.D., 1970. Depositional and dispersal dynamics of intertidal sand bars. Journal of Sedimentary Research 40 (4), 1095–1127.
Kleinhans, M.G., 2004. Sorting in grain flows at the lee side of dunes. Earth-Science Reviews 65 (1–2), 75–102.
Kneller, B.C., Branney, M.J., 1995. Sustained high-density turbidity currents and the deposition of thick massive beds. Sedimentology 42, 607–616.
Lee, C.H., 2019. Multi-phase flow modeling of submarine landslides: transformation from hyperconcentrated flows into turbidity currents. Adv. Water Resour. 131, 103383. https://doi.org/10.1016/j.advwatres.2019.103383.
Le Hir, P., Cayocca, F., Waeles, B., 2011. Dynamics of sand and mud mixtures: a multiprocess-based modelling strategy. Cont. Shelf Res. 31 (10), S135–S149.
Leppe, M., Mihoc, M., Varela, N., Stinnesbeck, W., Mansilla, H., Bierma, H., Cisterna, K., Frey, E., Jujihara, T., 2012. Evolution of the Austral-Antarctic flora during the Cretaceous: new insights from a paleobiogeographic perspective. Rev. Chil. Hist. Nat. 85, 369–392.
Leppe, M., Stinnesbeck, W., Hinojosa, L.F., Nishida, H., Dutra, T., Wilberger, T., Trevisan, C., Pino, J.P., Mansilla, H., Garrido, S., 2017. Paleoclimatic estimations in the Upper Cretaceous of Magallanes Region, Southern South America. In: 10th International Symposium on the Cretaceous. Agosto, Vienna, Austria.
Li, M., Amos, C.L., 1999. Field observations of bedforms and sediment transport thresholds of fine sand under combined waves and currents. Mar. Geol. 158, 147–160.
Loinaze, V.S.P., Vera, E.I., Raigemborn, M.S., Moyano-Paz, D., Santamarina, P., Agnolin, F., Manabe, M., Tsuihiji, T., Novas, F.E., 2025. Palynofloras from the Maastrichtian Chorrillo Formation (Patagonia, Argentina): paleoenvironmental and paleoclimatic implications. Palaeogeogr. Palaeoclimatol. Palaeoecol. 662, 112764.
Longhitano, S.G., Mellere, D., Steel, R.J., Ainsworth, R.B., 2012. Tidal depositional systems in the rock record: a review and new insights. Sediment. Geol. 279, 2–22.
Macellari, C.E., Barrio, C.A., Manassero, M.J., 1989. Upper Cretaceous to Paleocene depositional sequences and sandstone petrography of southwestern Patagonia (Argentina and Chile). J. South Am. Earth Sci. 2 (3), 223–239.
Malkowski, M.A., Schwartz, T.M., Sharman, G.R., Sickmann, Z.T., Graham, S.A., 2017. Stratigraphic and provenance variations in the early evolution of the Magallanes-Austral foreland basin: implications for the role of longitudinal versus transverse sediment dispersal during arc-continent collision. Bulletin 129 (3-4), 349–371.
Malumián, N., 1990. Foraminíferos de la Formación Man Aike (Eoceno, sureste lago Cardiel), Provincia de Santa Cruz. Rev. Asoc. Geol. Argent. 45 (3–4), 364–385.
Manríquez, L.M.E., Lavina, E.L., Fernández, R.A., Trevisan, C., Leppe, M.A., 2019. Campanian–Maastrichtian and Eocene stratigraphic architecture, facies analysis, and paleoenvironmental evolution of the northern Magallanes Basin (Chilean Patagonia). J. South Am. Earth Sci. 93, 102–118.
Manríquez, L.M.E., Lavina, E.L., Netto, R., Horodyski, R., Leppe, M., 2021. Evolution of a high latitude high-energy beach system (Maastrichtian–Eocene, Magallanes/Austral Basin, Chilean Patagonia). Sediment. Geol. 426, 106026. https://doi.org/10.1016/j.sedgeo.2021.106026.
Manríquez, L.M.E., Krahl, G., Carvalho, M.A., Lavina, E., Santiago, G., Bom, M., Fauth, G., Leppe, M., 2024. The K/Pg event at high southern latitudes: new evidence from continental deposits in the Magallanes/Austral Basin, Patagonia, South America. Cretac. Res. 162, 105931. https://doi.org/10.1016/j.cretres.2024.105931.
Marenssi, S.A., Casadío, S., Santillana, S.N., 2003. Estratigrafía y sedimentología de las unidades del Cretácico superior-Paleógeno aflorantes en la margen sureste del lago Viedma, provincia de Santa Cruz, Argentina. Rev. Asoc. Geol. Argent. 58 (3), 403–416.
Martinelli, A., Soto-Acuña, S., Goin, F.J., Kaluza, J., Bostelmann, J.E., Fonseca, P.H.M., Reguero, M.A., Leppe, M., Vargas, A.O., 2021. New cladotherian mammal from southern Chile and the evolution of mesungulatid meridiolestidans at the dusk of the Mesozoic era. Sci. Rep. 11, 7594. https://doi.org/10.1038/s41598-021-87245-4.
Martínez, L.C.A., Leppe, M., Manríquez, L.M.E., Pino, J.P., Trevisan, C., Manfroid, J., Mansilla, H., 2023. A unique Late Cretaceous fossil Wood assemblage from Chilean Patagonia provides clues to a high-latitude continental environment. Pap. Palaeontol. 9. https://doi.org/10.1002/spp2.1536.
Marzo, M., 1992. Sistemas fluviales de alta sinuosidad. In: Arche, A. (Ed.), Sedimentología. Nuevas Tendencias. CSIC, Madrid, pp. 107–141.
McCubbin, D.G., 1982. Barrier island and strand plain facies. In: Scholle, P., Spearing, D. (Eds.), Sandstone Depositional Environments, vol. 31. AAPG Memoir, pp. 247–279.
Meldahl, K.H., Scott, D., Carney, K., 1995. Autochthonous leaf assemblages as records of deciduous forest communities: an actualistic study. Lethaia 28 (4), 383–394.
Mella, P., 2001. Control tectónico en la evolución de la Cuenca de antepaís de Magallanes, XII Región, Chile. Memoria para optar al Título de Geólogo. Universidad de Concepción, Departamento de Ciencias de la Tierra (Inédito) 149.
Miall, A.D., 1996. The stratigraphic architecture of fluvial depositional systems. In: The Geology of Fluvial Deposits: Sedimentary Facies, Basin Analysis, and Petroleum Geology. Berlin Heidelberg, pp. 251–309.
Miall, A.D., 2000. Principles of Sedimentary Basin Analysis, third ed. Springer-Verlag Berlin Heidelberg, p. 616.
Miall, A.D., 2002. Architecture and sequence stratigraphy of Pleistocene fluvial systems in the Malay Basin, based on seismic time-slice analysis. AAPG Bull. 86 (7), 1201–1216.
Moscariello, A., 2018. Alluvial fans and fluvial fans at the margins of continental sedimentary basins: geomorphic and sedimentological distinction for geo-energy exploration and development. Geological Society, London, Special Publications 440 (1), 215–243.
Moyano-Paz, D., Tettamanti, C., Varela, A.N., Cereceda, A., Poiré, D.G., 2018. Depositional processes and stratigraphic evolution of the Campanian deltaic system of La Anita Formation, Austral-Magallanes Basin, Patagonia, Argentina. Lat. Am. J. Sedimentol. Basin Anal. 25 (2), 69–92.
Moyano-Paz, D., Rozadilla, S., Agnolin, F., Vera, E., Coronel, M.D., Varela, A.N., Gómez-Dacal, A.R., Aranciaga-Rolando, A.M., D'Angelo, J.S., Pérez-Loinaze, V., Richiano, S., Chimento, N.R., Motta, M.J., Sterli, J., Manabe, M., Takanobu, T., Isasi, M.P., Poiré, D.G., Novas, F.E., 2021. The Uppermost Cretaceous Continental Deposits (UCCD) at the Southern end of Patagonia, the Chorrillo Formation case study (Austral-Magallanes Basin): sedimentology, fossil content and regional implications. Cretac. Res., 105059 https://doi.org/10.1016/j.cretres.2021.105059.
Moyano-Paz, D., Rozadilla, S., Agnolin, F., Vera, E., Coronel, M.D., Varela, A.N., Gómez-Dacal, A.R., Aranciaga-Rolando, A.M., D'Angelo, J., Pérez-Loinaze, V., Richiano, S., Chimento, N., Motta, M.J., Sterli, J., Manabe, M., Tsuihiji, T., Isasi, M.P., Poiré, D.G., Novas, F.E., 2022. The uppermost Cretaceous continental deposits at the southern end of Patagonia, the Chorrillo Formation case study (Austral-Magallanes Basin): sedimentology, fossil content and regional implications. Cretac. Res. 130. https://doi.org/10.1016/j.cretres.2021.105059.
Mulder, T., Alexander, J., 2001. The physical character of subaqueous sedimentary density flows and their deposits. Sedimentology 48, 269–299.
Myrow, P., Southard, J., 1991. Combined-flow model for vertical stratification sequences in shallow marine storm-deposited beds. J. Sedimentary Research 61 (2), 202–210.
Nanson, G.C., Croke, J.C., 1992. A genetic classification of floodplains. Geomorphology 4, 459–486.
Natland, M.L., Gonzalez, E., Cañon, A., Ernst, M., 1974. A System of Stages for Correlation of Magallanes Basin Sediments. The Geological Society of America Memoir, Colorado, USA, p. 126.
Nichols, G., 2009. Sedimentology and Stratigraphy. John Wiley & Sons, p. 419.
Novas, F., Agnolin, F., Rozadilla, S., Aranciaga-Rolando, A.M., Brisson-Egli, F., Motta, M. J., Cerroni, M., Ezcurra, M., Martinelli, M., m D'Angelo, J., Alvarez- Herrera, G., Gentil, A., Bogan, S., Chimento, N., García-Marsa, J., Lo Coco, G., Miquel, S., Brito, F., Vera, E., Loinaze, V., Fernández, M., Salgado, L., 2019. Paleontological discoveries in the Chorrillo Formation (upper Campanian-lower Maastrichtian, Upper Cretaceous), Santa Cruz Province, Patagonia, Argentina. Revista del Museo Argentino de Ciencias Naturales 21 (2), 217–293.
Orem, W.H., Finkelman, R.B., 2003. Coal formation and geochemistry 7, 407pp.
Pemberton, S.G., Spila, M., Pulham, A.J., Saunders, T., MacEachern, J.A., Robbins, D., Sinclair, I.K., 2001. Ichnology and sedimentology of shallow to marginal marine systems: Ben Nevis & Avalon Reservoirs, Jeanne d'Arc Basin. Geological Association of Canada Short Course Notes 15, 343.
Perillo, M.M., Best, J.L., Garcia, M.H., 2014. A new phase diagram for combined-flow bedforms. J. Sediment. Res. 84, 301–313.
Pino, J.P., Leppe, M., Lobos, V., Wilberger, T., Trevisan, C., Ortuya, M.J., Manríquez, L., Garrido, S., Fernández, R., Hinojosa, L.F., Dutra, T., Nishida, H., 2016. Paleoclima del Cretácico Superior (Campaniano–Maastrichtiano) del Complejo Cerro Guido-Las Chinas, provincia de Última Esperanza, Chile: nuevas estimaciones a partir de improntas foliares. Abstracts, V Simposio de Paleontología de Chile, Concepción Chile 49–52.
Pyrcz, M.J., 2015. A review of some fluvial styles. Research Gate. Publication 237713953.
Püschel, H.P., Martinelli, A.G., Soto-Acuña, S., Ortiz, H., Leppe, M., Vargas, A.O., 2025. A subantarctic reigitheriid and the evolution of crushing teeth in these enigmatic Mesozoic mammals. Proceedings of the Royal Society B 292, 20251056.
Raigemborn, M.S., Lizzoli, S., Moyano-Paz, D., Varela, A.N., Poiré, D.G., Loinaze, V.S.P., Vera, E., Manabe, M., Tsuihiji, T., Sano, T., Novas, F.E., 2025. Maastrichtian climate of southern Patagonia (Argentina): an approach from paleosols of the dinosaur-bearing Chorrillo Formation. Cretac. Res. 174, 106144.
Ramón, J.C., Cross, T., 1997. Characterization and prediction of reservoir architecture and petrophysical properties in fluvial channel sandstones, middle Magdalena Basin, Colombia. C.T. F Ciencia, Tecnol., Futuro 1 (3), 19–46.
Reading, H.G., Collinson, J.D., 1996. Clastic coast. In: Reading, H.G. (Ed.), Sedimentary Environment: Processes, Facies and Stratigraphy. Blackwell Publishing, Oxford, pp. 154–231.
Reinhardt, J., 1980. Tuscaloosa Formation (Cenomanian) from eastern Alabama to central Georgia: its stratigraphic identity and sedimentology. Gulf Coast Section, SEPM Research Conference, Program and Abstracts, Houston, Texas, pp. 25–26.
Reinhardt, J., Smith, L.W., King Jr., D.T., 1986. Sedimentary Facies of the Upper Cretaceous Tuscaloosa Group in Eastern Alabama: Geological Society of America, SE Section, Field Guidebook, pp. 363–369.
Retallack, G.J., 2001. Soils of the past – an Introduction to Paleopedology, vol. 139. Unwin Hyman, London. Geological Magazine, pp. 97–104.
Rivera, H.A., Le Roux, J.P., Farías, M., Gútierrez, N., Sánchez, A., Palma-Heldt, S., 2020. Tectonic controls on the Maastrichtian-Danian transgression in the Magallanes-Austral foreland basin (Chile): implications for the growth of the Southern

Patagonian Andes. Sediment. Geol., 105645 https://doi.org/10.1016/j.sedgeo.2020.105645.
Ramos, A., Sopeña, A., 1983. Gravel bars in low-sinuosity streams (Permian and Triassic, central Spain). Modern and ancient fluvial systems, 301-312.
Romans, B.W., Fildani, A., Hubbard, S.M., Covault, J.A., Fosdick, J.C., Graham, S.A., 2011. Evolution of deep-water stratigraphic architecture, Magallanes Basin, Chile. Mar. Petrol. Geol. 28 (3), 612–628.
Scherer, C.M.S., Lavina, E., 2005. Sedimentary cycles and facies architecture of aeolian-fluvial strata of the Upper Jurassic Guará Formation, southern Brazil. Sedimentology 52, 1323–1341.
Scherer, C.M.S., Lavina, E., 2006. Stratigraphic evolution of fluvial-eolian sucession: the example of the Upper Jurassic-Lower Cretaceous Guará and Botucatu formations, Paraná Basin, Southern Brazil. Gondwana Res. 9, 475–484.
Scherer, C.M., Lavina, E.L., Dias Filho, D., Oliveira, F., Bongiolo, D., Aguiar, E., 2007. Stratigraphy and facies architecture of the fluvial–aeolian–lacustrine Sergi Formation (Upper Jurassic), Recôncavo Basin, Brazil. Sediment. Geol. 194, 169–193.
Schwartz, T.M., Graham, S.A., 2015. Stratigraphic architecture of a tide-influenced shelf-edge delta, Upper Cretaceous Dorotea Formation, Magallanes-Austral Basin, Patagonia. Sedimentology 62 (4), 1039–1077.
Schnurrenberger, D., Russell, J.M., Kelts, K., 2003. Classification of lacustrine sediments based on sedimentary components. J Paleolimnol 29, 141–154. https://doi.org/10.1023/A:1023270324800.
Schwartz, T.M., Fosdick, J.C., Graham, S.A., 2016. Using detrital zircon U-Pb ages to calculate Late Cretaceous sedimentation rates in the Magallanes-Austral basin, Patagonia. Basin Res. 29 (6), 725–746.
Smith, L.W., 1984. Depositional Setting and Stratigraphy of the Tuscaloosa Formation, Central Alabama to west-central Georgia. Unpublished MS Thesis. Auburn University, p. 125.
Smith, L.W., King Jr., D.T., 1983. The Tuscaloosa Formation: fluvial sedimentary facies, their correlation, and relationship to basement configuration. Alabama Geological Society, 20th Annual Field Trip Guidebook, pp. 21–25.
Smith, D.G., Hubbard, S.M., Leckie, D.A., Fustic, M., 2009. Counter point bar deposits: lithofacies and reservoir significance in the meandering modern Peace River and ancient McMurray Formation, Alberta, Canada. Sedimentology 56, 1655–1669.
Sohn, Y.K., 1997. On traction-carpets sedimentation. J. Sediment. Res. 67 (3), 502–507.
Soto-Acuña, S., Jujihara, T., Novas, F.E., Leppe, M., González, E., Stinnesbeck, W., Isasi, M.P., Rubilar-Rogers, D., Vargas, A.O., 2014. Hadrosaurios (Ornithopoda: Hadrosauridae) en el Cretácico Superior Del Extremo Austral De América Del Sur. Abstracts, IV Simposio Paleontología En Chile. Universidad Austral de Chile, Valdivia, p. 56.
Soto-Acuña, S., Alarcón-Muñoz, J., Fernández-Jiménez, R., Guevara, J.P., González, E., Manríquez, L., Jujihara, T., Rubilar-Rogers, D., Vargas, A.O., Leppe, M., 2016a. Primer registro de titanosaurios (Sauropoda: Lithostrotia) de la Región de Magallanes, extremo sur de Chile. Abstracts, V Simposio de Paleontología en Chile, Concepción 146.
Soto-Acuña, S., Alarcón, J., Guevara, J.P., Fernández, R., González, E., Leppe, M., Vargas, A.O., 2016b. Nuevos hallazgos de reptiles marinos en la Formación Dorotea (Maastrichtiano) de la región de Magallanes, extremo austral de Chile. Ameghiniana 53 (6 Suppl. o), 76 R.
Soto-Acuña, S., Vargas, A.O., Kaluza, J., Leppe, M.A., Botelho, J.F., Palma-Liberona, J., Simon-Gutstein, C., Fernández, R.A., Ortiz, H., Milla, V., Aravena, B., Manríquez, L. M., Alarcón-Muñoz, J., Pino, J.P., Trevisan, C., Mansilla, H., Hinojosa, L.F., Muñoz-Walther, V., Rubilar-Rogers, D., 2021. Bizarre tail weaponry in a transitional ankylosaur from subantarctic Chile. Nature 600, 259–263.
Spackman, W., 1974. A field guidebook to aid in the comparative study of the Okefenokee Swamp and the Everglades-mangrove swamp-marsh complex of southern Florida. Geological Society of America.
Suazo, F., Gómez, R.O., 2021. In the shadow of dinosaurs: Late Cretaceous frogs are distinct components of a widespread tetrapod assemblage across Argentinean and Chilean Patagonia. Cretac. Res., 105085 https://doi.org/10.1016/j.cretres.2021.105085.
Talbot, M.R., Allen, P.A., 1996. Lakes. In: Reading, H.G. (Ed.), Sedimentary Environments: Processes, Facies, and Stratigraphy. Blackwell Science, Oxford, pp. 83–124.
Taylor, J.E., Whitelaw, C.A., 2001. Signals in abscission. New Phytol. 151 (2), 323–340.
Tettamanti, C., Moyano Paz, D., Varela, A.N., Tineo, D.E., Gómez-Peral, L.E., Poiré, D.G., Cereceda, A., Odino Barreto, A.L., 2018. Sedimentology and Fluvial Styles of the Uppermost Cretaceous Continental deposits of the Austral-Magallanes Basin, Patagonia, Argentina. Lat. Am. J. Sedimentol. Basin Anal. 25 (2), 149–168.
Thomas, B.A., Cleal, C.J., Kuhrmann, M.H., Hemsley, A.R., 1999. Abscission in the Fossil Record. the Evolution of Plant Architecture. Royal Botanic Gardens, Kew, pp. 183–203.
Trevisan, C., Dutra, T., Wilberger, T., Leppe, M., Manríquez, L., 2020. An austral fern assemblage from the Upper Cretaceous (Campanian) beds of Cerro Guido, Magallanes Basin, Chilean Patagonia. Cretac. Res. 106, 104215. https://doi.org/10.1016/j.cretres.2019.104215.
Van de Meene, J.W.H., Boersma, J.R., Terwindt, J.H.J., 1996. Sedimentary structures of combined flow deposits from the shoreface-connected ridges along the central Dutch coast. Mar. Geol. 131 (3-4), 151–175.
Varela, A.N., Richiano, S., Paz, D.M., Tettamanti, C., Poiré, D.G., 2019. Sedimentology and stratigraphy of the Puesto El Moro Formation, Patagonia, Argentina: implications for upper cretaceous paleogeographic reconstruction and compartmentalization of the Austral-Magallanes Basin. J. South Am. Earth Sci. 92, 466–480.
Vera, E.I., Loinaze, V.S.P., Moyano-Paz, D., Coronel, M.D., Manabe, M., Tsuihiji, T., Novas, F.E., 2022. Paleobotany of the uppermost Cretaceous Chorrillo Formation, Santa Cruz Province, Argentina: insights in a freshwater floral community. Cretac. Res. 138, 105296.
Wang, Y., Mosbrugger, V., Zhang, H., 2005. Early to Middle Jurassic vegetation and climatic events in the Qaidam Basin, Northwest China. Palaeogeogr. Palaeoclimatol. Palaeoecol. 224 (1-3), 200–216.
Wakelin-King, G.A., Webb, J.A., 2007. Upper-flow-regime mud floodplains, lower-flow-regime sand channels: sediment transport and deposition in a drylands mud-aggregate river. J. Sediment. Res. 77 (9), 702–712.
Willis, B. J. 2005. Deposits of tide-influenced river deltas.
Willis, J.B., Tang, H., 2010. Three-dimensional connectivity of point-bar deposits. J. Sediment. Res. 80, 440–454.
Wilson, T., 1991. Transition from back arc to foreland basin development in the southern Andes: stratigraphic record from the Ultima Esperanza District, Chile. Geol. Soc. Am. Bull. 103, 98–111.
Wood, G.D., Gabriel, A.M., Lawson, J.C., 1996. Chapter 3. Palynological techniques — processing and microscopy. In: Jansonius, J., McGregor, D.C. (Eds.), Palynology: Principles and Applications, vol. 1. American Association of Stratigraphic Palynologists Foundation, Dallas, pp. 29–50.
Wright, V.P., Marriott, S.B., 2007. The dangers of taking mud for granted: lessons from Lower Old Red Sandstone dryland river systems of South Wales. Sediment. Geol. 195 (1-2), 91–100.